# Copyright Warning & Restrictions

The copyright law of the United States (Title 17, United States Code) governs the making of photocopies or other reproductions of copyrighted material.

Under certain conditions specified in the law, libraries and archives are authorized to furnish a photocopy or other reproduction. One of these specified conditions is that the photocopy or reproduction is not to be "used for any purpose other than private study, scholarship, or research." If a, user makes a request for, or later uses, a photocopy or reproduction for purposes in excess of "fair use" that user may be liable for copyright infringement,

This institution reserves the right to refuse to accept a copying order if, in its judgment, fulfillment of the order would involve violation of copyright law.

Please Note: The author retains the copyright while the New Jersey Institute of Technology reserves the right to distribute this thesis or dissertation

Printing note: If you do not wish to print this page, then select "Pages from: first page # to: last page #" on the print dialog screen

## ABSTRACT

**Measurement of Dynamic Friction**

by
Atif Aly

The friction force between two bodies sliding at constant relative velocity is a function of their relative velocity. Under conditions of time-variable relative velocity, the instantaneous friction is a function not only of the instantaneous velocity but also the velocity history. An understanding of the resulting dynamic friction function will allow for the design of control systems where velocity is time-varying, oscillatory and often contained in a relatively small region centered around zero amplitude. Within the control system, a portion of the control force can be implemented to effectively counteract the friction present and allow for precise motion control.

In this thesis a theoretical model which simulates the dynamic friction function requires verification through comparison with experimental data. An electro-mechanical system was designed and implemented to achieve this aim. The present system allows for the control of various parameters such as test-shaft angular frequency and velocity, test-shaft applied loan and lubricating oil viscosity. The subsequent comparison of theoretical and experimental data enables us to estimate the integrity of the model and offers insight into areas which require further investigation.

# DYNAMIC FRICTION MEASUREMENT

by
Atif Aly

A Thesis
Submitted to the Faculty of
New Jersey Institute of Technology
in Partial Fulfillment of the Requirements for the Degree of
Master of Science in Mechanical Engineering

Department of Mechanical
and Industrial Engineering

May 1994

APPROVAL PAGE

DYNAMIC FRICTION MEASUREMENT

Atif Aly

Dr. Avraham Harnoy, Thesis Advisor — Date
Associate Professor of Mechanical Engineering, NJIT

Dr. Ernest S. Geskin, Committee Member — Date
Professor of Mechanical Engineering, NJIT

Dr. Rong-Yaw Chen, Committee Member — Date
Professor of Mechanical Engineering, NJIT

## BIOGRAPHICAL SKETCH

**Author:** Atif Ahmad Aly

**Degree:** Master of Science in Mechanical Engineering

**Date:** May, 1994

**Undergraduate and Graduate Education**

- Master of Science in Mechanical Engineering
  New Jersey Institute of Technology
  Newark, New Jersey, 1994
- Bachelor of Science in Mechanical Engineering
  Cairo University
  Cairo, Egypt, 1982

**Major:** Mechanical Engineering

## ACKNOWLEDGMENT

I express my appreciation to Dr. Avraham Harnoy, Associate Professor in the Department of Mechanical Engineering, New Jersey Institute of Technology for his guidance and suggestion in preparation of this thesis.

Particular acknowledgment to the Mechanical Engineering workshop for their help in designing and construction of the measuring system.

Also appreciation to the student Richard Semenock for his help in running the experiments.

Finally I wish to thank my family who encouraged me to stay and finish my studies.

TABLE OF CONTENTS

TABLE OF CONTENTS

(Continued)

# CHAPTER 1

## INTRODUCTION

The object of the present study is to develop an experimental testing machine to measure the dynamic friction in hydrodynamic journal bearings. In order to have precise motion control, one option is to minimize the friction in the design, using low friction bearing, or using contactless technique in which the surfaces are completely separated at all velocities, including zero velocity. These techniques are almost always expensive, and in some application, they are not feasible. The second possibility is to consider the friction function during the design process of the central system. If the force due to friction is smaller in magnitude than the maximum available control force, one possibility would be to use a portion of the control force to counteract the effect of friction.

Many bearing-testing machines, now in effective use are built around the idea of eliminating internal friction. The machine built by Texas Company for general-purpose testing and research use is called a universal bearing-testing machine. Figure 1.1 shows the method for applying load to the test bearing and for measuring the bearing friction. Load is introduced by means of

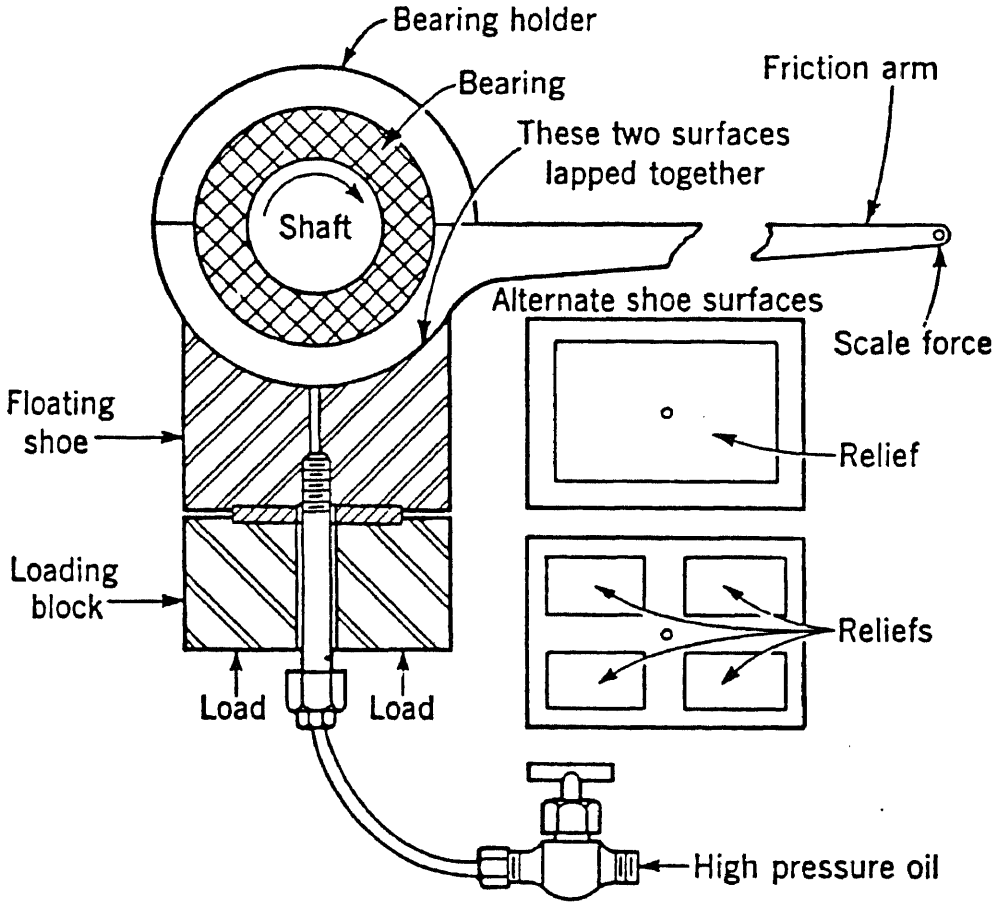


**Figure 1.1** Universal bearing-testing machine

a hydraulic cylinder and yoke to the bottom of the bearing through a loading block. As the shaft turns, the frictional torque between shaft and bearing is evaluated by measuring the force exerted against a weighing scale placed at the end of the friction arm. By applying high-pressure oil to a set of reliefs at the surface between the shoe and bearing holder,

the two surfaces can be separated and the frictional drag reduced effectively to zero.

In 1988 a machine was built by Moshe David to examine the influence of polymer additives on journal bearing performance under static load. The angle of friction was measured by the displacement of the weight connecting rod, using an indicator (dial gauge) as shown in Figure 1.2. The speed components were measured by a tachometer attached to the journal.

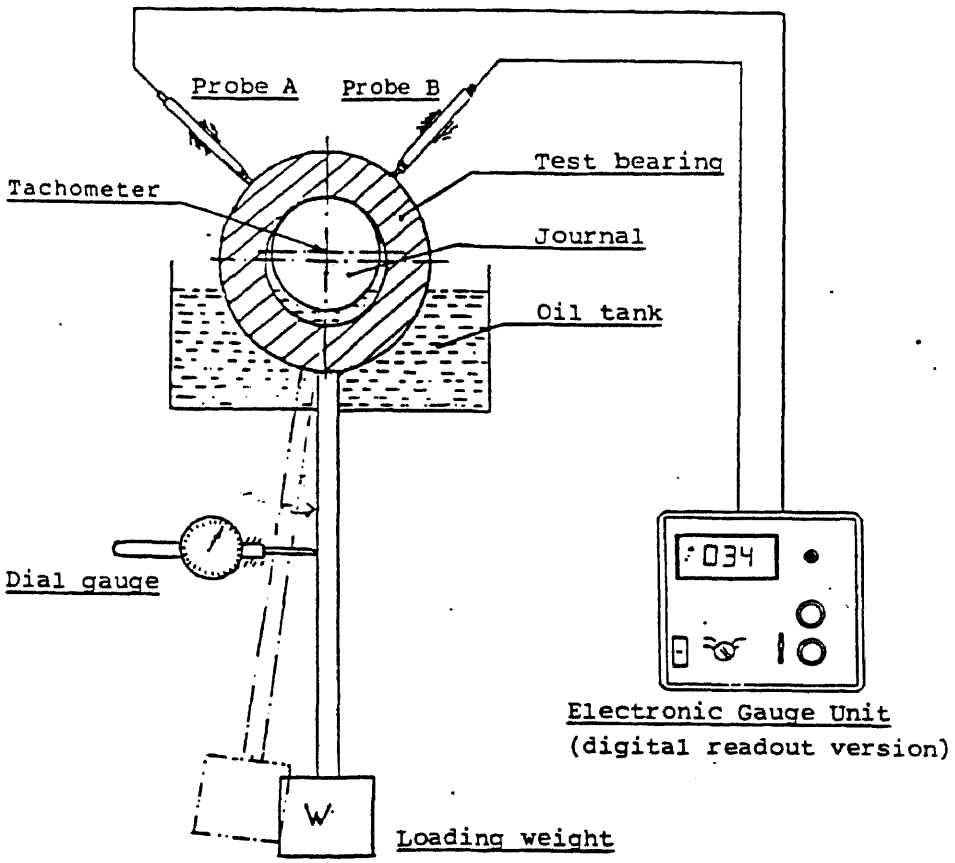


**Figure 1.2** Instrumentation set-up for measuring journal bearing performance

With the testing machine in question, unlike all previous machines, it is more precise to measure dynamic friction. In this machine we used a servo-motor to drive the test shaft with a pre-determined voltage wave. The resulting strain and shaft velocity signals are processed and finally recorded by the computer system. These recorded values are used to render a graph of friction. Torque vs. shaft velocity.

# CHAPTER 2

## HYDRODYNAMIC LUBRICATION

The first investigations of hydrodynamic behavior were carried out towards the end of the nineteenth century. As early as 1874, Stefan in Germany investigated the squeeze behavior of a lubricant confined between approaching plane surfaces. Beauchamp Tower conducted experiments in England to determine the friction of the journal of a railway-car wheel, and observed the generation of hydrodynamic pressure in the first partial journal bearing. The pressures generated even in these early experiments of 1885 were sufficiently large to displace plugs or stoppers placed in oil holes in the bearing casing.

The hydrodynamic theory of lubrication is based primarily upon a rather complicated mathematical analysis of the motion of fluids, including semi-solids, liquids and gases. The hydrodynamic theory of lubrication is applied everywhere to many thousands of bearings and machine elements so as literally to keep the wheels of our great and ponderous civilization turning at top speed.

The hydrodynamic theory may also be used to design and analyze certain pumps, develop precision gaging apparatus, and in computer memory systems, and has been used in a ruling engine to maintain the alignment of the translating bed to within a few millionths of an inch.

## 2.1 Development of Hydrodynamic Theory

The assumptions underlying the theory of hydrodynamic lubrication as originally proposed by Reynolds in 1886, are as follows:

(a) Neglect of gravitation and inertia terms.

(b) Assumption of Newtonian behavior.

(c) Constant viscosity.

(d) Incompressibility of fluid.

(e) Film thickness small compared with other dimensions.

(f) Zero slip at liquid-solid or gas-solid boundaries.

(g) No surface tension effects.

The (f) and (g) assumptions are usual ones in fluid mechanics, and the neglection of inertia in the first assumption is made possible by (e). As a consequence of the latter, velocity components in the z-direction may be neglected. The conditions of isoviscosity, incompressibility, and Newtonian behavior have been removed by subsequent refinements and extensions to the original theory.

## 2.2 Hydrodynamic Lubrication of Journal Bearing

Journal bearing is viewed as a slider bearing in which the film thickness has variation associated with the distance between the eccentric cylinders as shown in Figure . The approach is to be concerned first with the minimum film thickness in the bearing as it is running. If the film becomes too thin, metal-to-metal contact will be initiated and the bearing will destroy itself. Secondly, the engineer is

concerned with friction loss in the bearing to estimate the friction horsepower that will be expended and determine the heat that must be removed from the bearing in order to maintain its temperature at a reasonable steady state level. Thirdly, the amount of oil supply required by the bearing must be evaluated.

When starting with metallic contact between the shaft and bearing at a point under the load, the shaft will start to run in the right side of the bearing toward point B, and after rising a few degrees of arc, it will enter a region where oil comes between the bearing and the journal. Slip will begin, as the journal comes up to speed. It will revolve faster and build up a wedge-shaped film which placed the journal in the position shown.

The film thickness at the point of closest approach is designated as ho. A negative pressure will be established in the crown of the bearing and will contribute very little to the load carrying function of the bearing since the positive oil film pressures are generally many orders of magnitude larger than these negative pressures. Point O represents the center of the bearing and O′ the center of the shaft. The radius of the shaft is r, and the radius of the bearing R. Distance between O and O′ is indicated by a and is the eccentric distance. The ratio of a for the actual operating conditions to the radial clearance in the bearing and is called eccentricity ratio e.

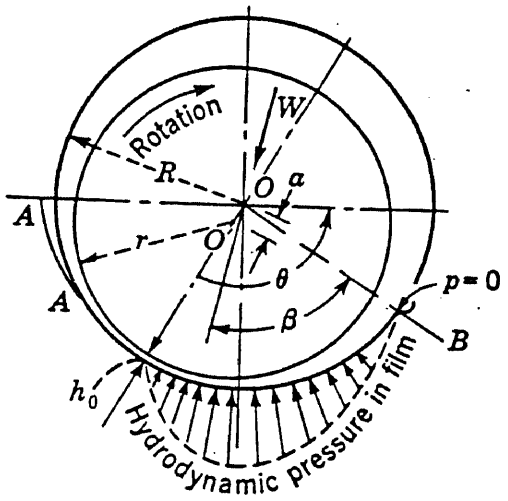


**Figure 2.1** Journal in 360 full bearing

### 2.3 Hydrodynamic Force

The assumption of Dubois and Ocvirk for a short journal bearing operating at steady speed are extended for dynamic and mixed region conditions. The pressure gradients in the x (circumferential) direction are neglected since they are very small compared with gradients in the 2 (axial) direction as shown in Figure 2. Also the pressure distribution at o o n is considered only for fluid film force calculations, where the pressure is above the atmospheric.

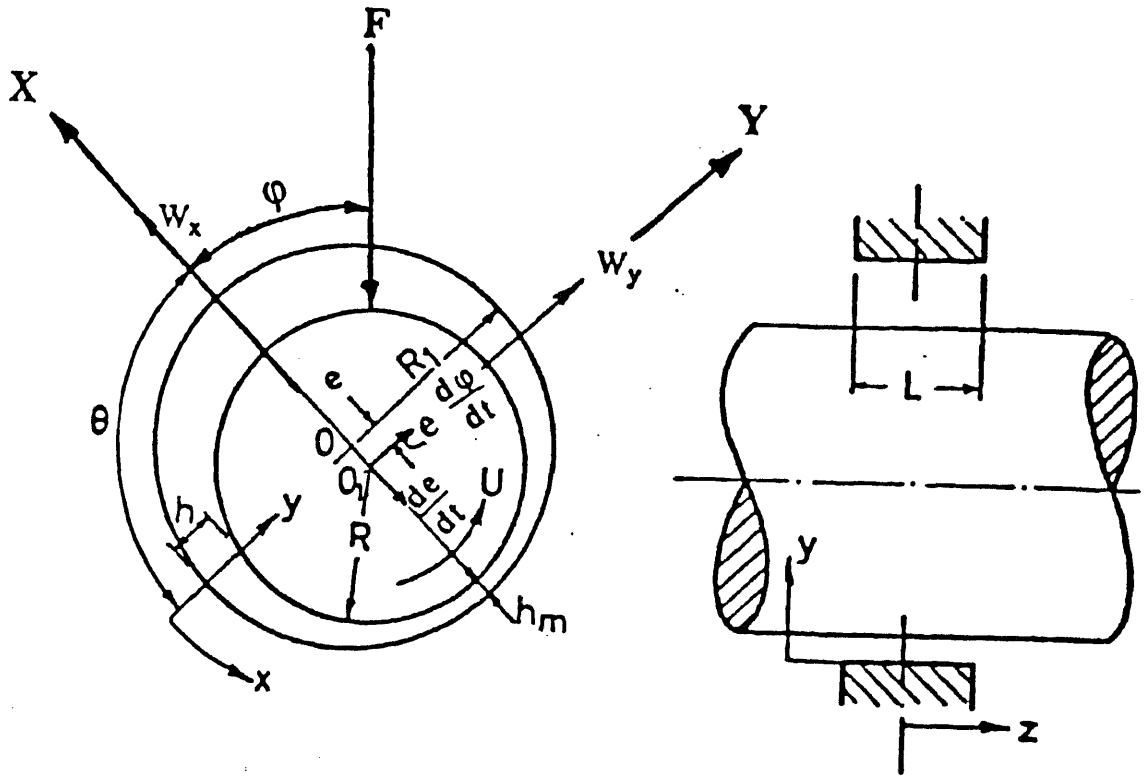


**Figure 2.2** Short journal bearing

The conventional assumption of Reynold's classical hydrodynamic theory is maintained. Since the mass of the fluid is very small, the effect of fluid inertia can be neglected. However, the journal mass is considered as its magnitude and is a few orders higher than the fluid mass. The

hydrodynamic pressure distribution P under dynamic conditions is derived from the following Reynold's equation for a thin incompressible fluid film (See Szeri, A-Z).

$$\frac{1}{6\mu}\left[\frac{\partial}{\partial x}\left(h^3\frac{\partial P}{\partial x}\right)+\frac{\partial}{\partial z}\left(h^3\frac{\partial P}{\partial z}\right)\right] = (U_j-U_s)\frac{\partial h}{\partial x}+2V_j \qquad (2.1)$$

where Vj is the journal surface radial velocity, opposite to the y direction, that squeezes the fluid film and Uj, Us are circumferential velocities of the journal and the sleeve respectively.

Integrating equation (2.1) twice, together with the boundary conditions of film for velocity and pressure results in the pressure distribution P for an unsteady, short hydrodynamic hearing:

$$P=\frac{3}{4}\frac{\mu L^3}{C_2}\left\{(\omega_j+\omega_s)\,\varepsilon\sin\theta-2\varepsilon\frac{d\varphi}{dt}\sin\theta-2\frac{d\varepsilon}{dt}\cos\theta\right\}\frac{L^2-4z^2}{h^3} \qquad (2.2)$$

where h is a variable film thickness around the bearing E

$$h= CE\ (1+\cos o) \qquad (2.3)$$

The fluid film force components Wx, Wy are obtained by integrating the pressure distributed in the converging clearance o o n

$$W_x = \frac{\mu RL^3}{C^2}\left\{-\frac{1}{2}J_{12}\varepsilon\left(\frac{d\theta_j}{dt}+\frac{d\theta_s}{dt}\right)+J_{12}\varepsilon\frac{d\varphi}{dt}+J_{22}\frac{d\varepsilon}{dt}\right\} \qquad (2.4)$$

$$W_y = \frac{\mu RL^3}{C^2}\left\{\frac{1}{2}J_{11}\varepsilon\left(\frac{d\theta_j}{dt}+\frac{d\theta_s}{dt}\right)-J_{11}\varepsilon\frac{d\varphi}{dt}-J_{12}\frac{d\varepsilon}{dt}\right\} \qquad (2.5)$$

The integrals Jij occurring in Equation (2.4, 2.5) are given by:

$$J_{11} = \int_0^{\pi} \frac{\mathrm{Sin}^2\theta}{(1+\varepsilon\,\mathrm{Cos}\theta)^3}\,d\theta = \frac{\pi}{2(1-\varepsilon^2)^{\frac{3}{2}}} \qquad (2.6)$$

$$J_{12} = \int_0^{\pi} \frac{\mathrm{Sin}\theta\,\mathrm{Cos}\theta}{(1+\varepsilon\,\mathrm{Cos}\theta)^3}\,d\theta = \frac{-2\varepsilon}{(1-\varepsilon^2)^2} \qquad (2.7)$$

$$J_{22} = \int_0^{\pi} \frac{\mathrm{Cos}^2\theta}{(1+\varepsilon\,\mathrm{Cos}\theta)^3}\,d\theta = \frac{\pi}{2}\,\frac{(1+2\varepsilon^2)}{(1-\varepsilon^2)^{\frac{5}{2}}} \qquad (2.8)$$

## 2.4 Applications of Hydrodynamic Theory

The main application for geometric shape and that which is typical of the journal bearing is to destroy the oil film in the bearing and introduce high friction in an oil ring as shown in (Figure 2.3). The journal motion drags the ring through the oil in the sump and raises the oil to the top of the bearing,. More oil is delivered due to the rotation of the ring at high speed, if the frictional driving force is increased at the point of contact between the top of the shaft and the inside of the oil ring.

This is done by deliberately grooving the inside surface of the ring to break down the oil film that would normally be created.

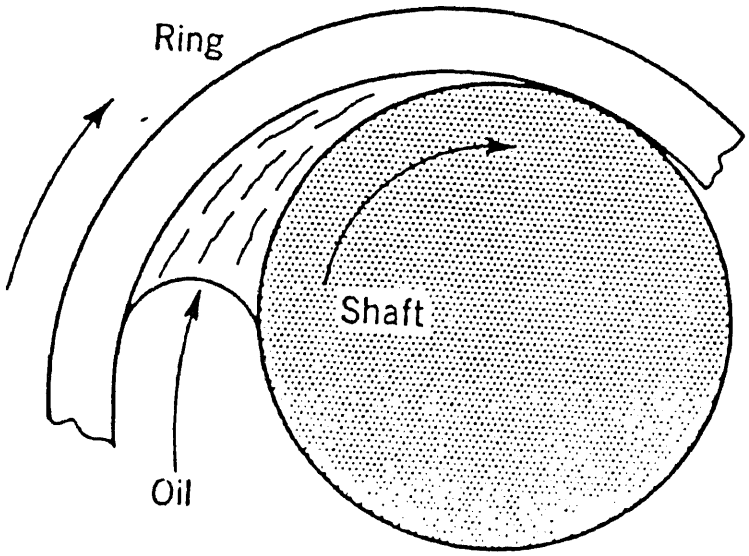


**Figure 2.3** Detail of film formation between ring and shaft

The second application comes from one engineer who wants to make two parallel axial groves in the bottom of the journal bearing. The diameter of the bearing was about 18 inches.

There was a special reason for the presence of these grooves in the bearing, placed three inches apart as shown in (Figure 2.3).

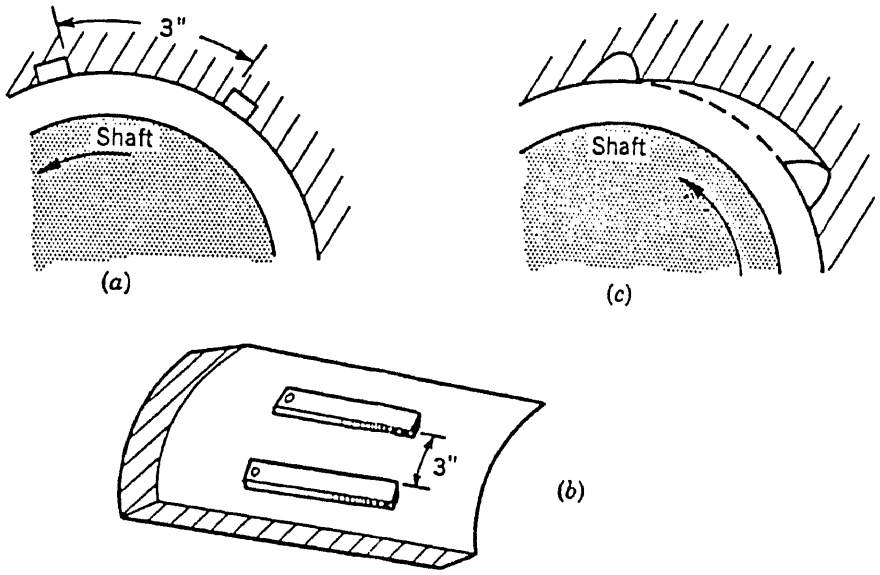


**Figure 2.4** Grooved journal bearing

So as to produce the least interference with the load-carrying capacity of the bearing, this engineer decided to taper the area between the grooves, so that this area might act like a tapered-land thrust bearing. But the slope was too great. It was about 1/16th of an inch in 3 inches and the bearing failed when it was place in service. The taper was too steep to build up a fluid film pressure, and effectively then a groove 3 inches wide had been placed in the bottom of

the bearing which caused it to fail. On a minute scale, shallow pits or indentations will tend to act as tiny tapered-land bearings and help maintain an oil film.

# CHAPTER 3

# DRY FRICTION

The theoretical analysis of the friction mechanism between a projection and the surface with perfect smoothness, both modeled to represent a certain surface roughness, has so far been attempted. Shapes of projections used for theoretical analyses include circular cone, hemisphere and triangular or regular pyramid and the other shapes.

If we slide one solid body over another, there is a resistance to this motion. This resistance is called friction. Frequently friction is considered a nuisance, and from earliest times man has made ingenious attempts to eliminate it or to reduce it as much as possible. The real damage occurs through wear or seizure of some vital machine part.

High friction between automobile tires and roadway is an obvious measure of safety in coming to a quick stop. Of course, without friction in brake shoes, or on railroad rails, or for that matter between the sidewalk and our shoes, life would indeed be very difficult.

## 3.1 Types of Friction

There are several types of friction:

a. Dry: static and kinetic.

b. Boundary: static and kinetic.

c. Fluid Friction

d. Semifluid or Mixed Friction

### 3.2 Dry Friction

Experiments on friction were carried out by Leonardo da Vinci (1452-1519). He recorded drawings of a rectangular block sliding over a plane surface and from his experiments deduced certain laws regarding the friction of the block. He wrote, "The friction made by the same weight will be of equal resistance at the beginning of the movement, although contact may be of different breadths or lengths." Da Vinci also observed, "Friction produces double the amount of effort if the weight be doubled."

Static friction is a measure of the force required to start motion or start sliding, where kinetic friction is a measure of the force required to maintain motion. Decrease in friction is gradual as velocity gets higher.

To study frictional properties between the soft material having particular surface asperities organized in the cutting direction caused by the method of manufacturing (e.g, lathe or shaper) and the hard material (covered with hard projections) finished by a grinding machine or the like, a contacting model was constructed between two kinds of projections modeled on the surface of the hard and the soft materials, respectively. On the basis of this model, a theoretical analysis of dry frictional properties was attempted. The projections were modeled as triangular prisms arranged in parallel with a

cutting direction on the soft material and as circular conical projections on the hard material. The theoretical analysis based on this contacting model was done taking into consideration the two kinds of frictional resistance caused by the ploughing and shearing.

Amontons-Coulomb(1699) evaluated the frictional forces between solids he said that the coefficient of friction was equal to the frictional force divided by the load.

$$F=fW \qquad (3.1)$$

The Amontons-Coulomb laws of dry friction are recognized as follows:

1. The friction force is directly proportional to the load.

2. The friction force is independent of the gross area of the contacting surfaces.

3. The friction force depends upon the nature of the sliding surfaces.

4. The friction force is independent of the siding velocity.

Thus the rougher the surface, the greater is the friction, and conversely the smoother the surface, the lower is the friction. This explanation of friction is generally accurate for relatively rough surfaces. The limiting case of low friction would be two extremely smooth surfaces in contact which, according to Coulomb, should have very low friction.

### 3.3 Concept of Friction

It is generally agreed that even the best surfaces are not the smooth. even for very finest smoothest commercial surfaces show an rms roughness on the profilomoter of about 0.5 to one millionth of an inch. The greatest height of peak over valley is even larger than this.

It is a very difficult to make a surface completely flat. Even on carefully polished surfaces, valleys and hills are present which are very large in comparison with the size of the molecule.

To determine what is the real area of contact between solids, the methods used have been varied. Sections have been cut through specimens and observed under the microscope. To increases the sensitivity of the method by simply technique. If, instead of cutting the section at 90 degrees to the surface, it is cut at an angle of fewer degrees, the effect is to magnify the irregularities in the vertical direction by a factor of ten or so, leaving the horizontal magnification unchanged.

From all of these measurements, it is clear that the real area of contact between solids is very small. Putting two solids together is, according to Bowden, "like turning Switzerland upside down and standing it on Austria."

When two such surfaces are pressed together the load is carried on just a few points (Figure 3-1). These are subjected to heavy unit pressures, and so they probably weld together. The energy necessary to break these welds is

transformed into heat, the temperature rises, and the welding process becomes more rapid and extensive.

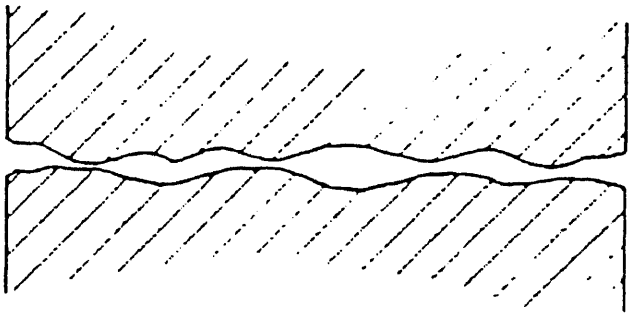

**Figure 3.1** Real contact of smooth solids

Another test shows that the amount of pick-up is directly proportional to the normal load. This means that the number

of welded junctions is proportional to the load.

An important observation can be made from these tracer techniques. Pick-up for dissimilar metals is 10 to 100 times less than that observed with similar metals, although the coefficient of friction is not very much smaller. This suggests that for dissimilar metals the junctions or welds are somewhat weaker and tend to shear at the actual interface. This would reduce abrasion, wear, and general metallic pick-up.

A good boundary lubricant does two things:

(1) It reduces friction between metal surfaces by a factor of as much as 20; but

(2) It reduces pick-up by a factor of 20,000 or more. Thus we see directly that metallic transfer is immensely more sensitive to changes in the condition of the surfaces than is the coefficient of friction.

## 3.4 Variables in Friction

*Cleanliness and Surface Films*

When solids are cleaned in air, their surfaces are still covered with a thin film of oxide, water vapor, and other adsorbed impurities. The contaminant film is usually at least several molecular layers in thickness, and any complete theory of friction must take this film into consideration.

Earlier experiments have not recognized the presence of this film, which represented one of the principal contributions to the difficulty of reproducing results. You

remove the grosser surface contamination by heating the metal surfaces in a vacuum.

*Effect of Velocity and Temperature*

As the velocity of sliding increases from zero to a finite value, friction usually reduces. As the velocity of sliding continues to increase, the friction in general continues to fall but not as rapidly. At high sliding speeds it may be the temperature that influences friction more than the sliding velocity. However, the overall effect of sliding velocity (and temperature) does exist. The problem of the effect of friction upon the motion of a bullet in a gun barrel has for a long time puzzled those who are especially interested in gun design and ballistics. As the speed of the bullet increases with non-uniform acceleration from zero to a muzzle velocity of as much as 3000 ft/sec, the friction falls.

Friction at high sliding velocities is also important to the designer of any vehicle that is to be stopped by the application of a brake. Galton and Westinghouse executed a most remarkable series of tests on the action of railroad brakes. By pneumatic and mechanical means they equipped a test car with instruments to record, as a function of time, normal brake force on shoes, tangential brake force on shoes, draw bar pull on car, and instantaneous forward velocity.

A summary of the results of Galton and Westinghouse is that the absolute values of the coefficient of friction are probably representative of those to be expected under actual railroad operating conditions, as the surfaces were most

certainly subjected to severe contamination from roadbed dust and dirt.

Prolonged application of brakes on road vehicles, as when descending a long mountainous grade, usually results in "fading" of the braking effect as the temperature of the lining continues to rise. This is especially serious with trucks. Drum temperature up to 400 degrees F are quite common, and on long downgrades truck drum temperatures as high as 700 degrees F have been recorded.

The drum temperatures of a passenger car can easily reach 400 degrees F after a stop from 60 mph. This is not surprising if one considers the amount of energy that must be absorbed by the comparatively small area of the braking surface.

As the temperature rises to 300 degrees F, there is a small drop in the coefficient of friction. If the temperature continues to rise to say 500 degrees F, there may be an increase in friction caused by the deterioration of the surface of the brake lining.

# CHAPTER 4

## BOUNDARY LUBRICATION

When a machine is started from rest, however, it often happens that the bulk of the intervening lubricant has been squeezed out during the idle period, and only an adherent surface film remains. This film may be only a few molecules think, but it can still prevent seizure of the parts and permit sliding to take place. The adherent film of lubricant is bounded to the metal substrate by very strong molecular adhesion forces and it has obviously lost its bulk fluid properties. Boundary lubrication is present during the running in process of most lubricated moving surfaces. This is the wearing-in condition when high spots or asperities of the mating surfaces are abraded or worn off. Figure 4.1 shows the well known Stribeck curve of friction coefficient vs. steady sliding velocity between lubricated sliding surfaces, including hydrodynamic journal bearings.

Below the transition velocity Utr the Stribeck curve shows the mixed lubrication region where the thickness of the lubrication film is less than the maximum size of the surface asperities. Under load, there is a contact between the surfaces, resulting in elastic as well as plastic deformation of the asperities. The film thickness increases with velocity; therefore, as the velocity increases a larger friction of external load is carried by the fluid film. The

result is that the friction decreases with velocity in mixed region because the fluid viscous friction is lower than the mechanical friction at contact between asperities.

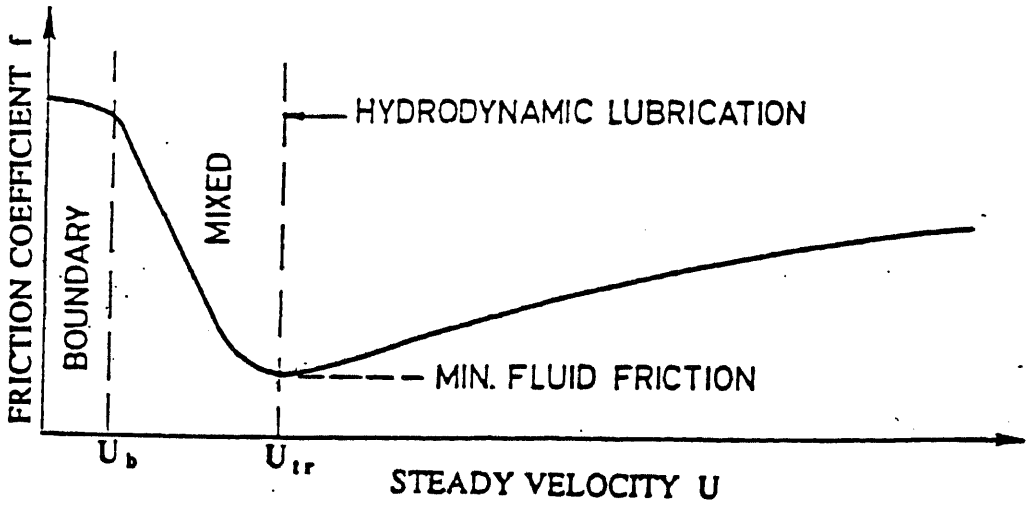


**Figure 4.1** Stribeck curve -
friction coefficient vs. steady velocity

### 4.1 Molecular Structure of Boundary Lubrication

The majority of lubricants are oils that are compounds of carbon and hydrogen with perhaps a small amount of other elements. There are two main categories; vegetable oils and mineral oils. Vegetable oils are mixtures of a wide variety of substances, including chiefly tri-glycerides and then fatty acids and esters as shown in Figure 4.2 The tri-glycerides have three long carbon chains hooked through a carboxyl linkage to a nucleus of three carbon atoms. Fatty acids and esters are essentially long-chain carbon atoms (again with hydrogens attached); the former having a hydroxy (-OH) or a carboxyl (-COOH) radial on one end.

The action of fatty acids in reducing friction under boundary conditions is now generally agreed to be one of molecular adherence. The fatty acid adheres to the surface with sufficient strength to resist being torn off when the rubbing surfaces slide over each other. It has been shown that the molecules of fatty acids have carboxyl groups that attach themselves to the metal surface.

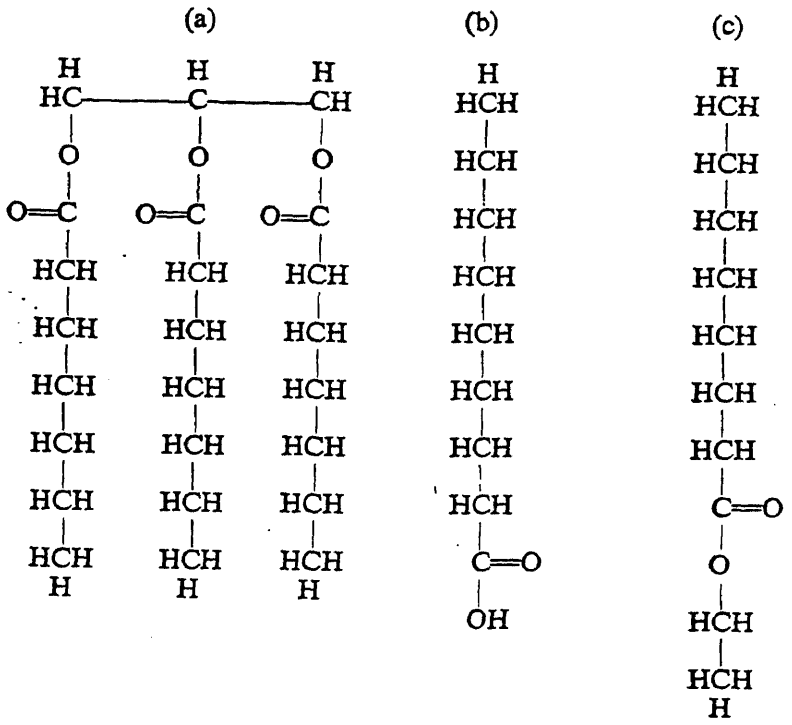


**Figure 4.2** Molecular structure of vegetable oils (a) A tri-glyceride; (b) a fatty acid and (c) an ester

The molecules of mineral oils are generally in the shape of long chains of carbon atoms with hydrogens attached, or of rings with long side chains as shown in Figure 7.3 The relatively high viscosity that oils possess can be pictured physically as due to the entangling and intermeshing of their very long chains. Also a tendency for chains under certain conditions to align themselves parallel to one another or perhaps to pack closely together, thus forming the relatively dense and rigid layer on a solid surface.

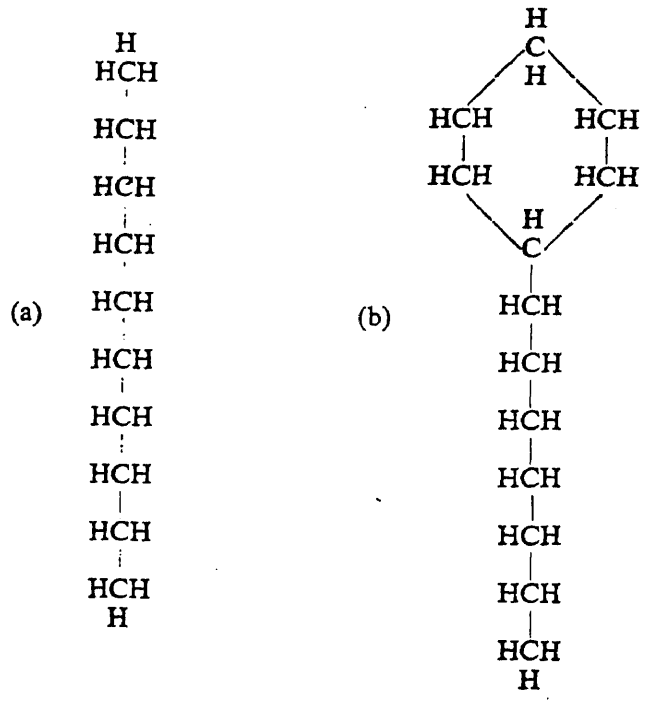


**Figure 4.3** Molecular structure of mineral oils

Generally unsaturation is likely to occur in vegetable oils and saturation in mineral oils. The region of the double bond is chemically active and will absorb other molecules, notably oxygen from the air, if the oil is heated. This phenomenon has two results:

(a) oxidation produces gum and varnish deposits which are usually harmful in engines; and

(b) it produces acidity of the oil, and leads to severe

chemical attack of bearing surfaces.

All of the molecular structures shown in Figures 7.2, 7.3 have a common feature, namely a long chain.

## 4.2 Additives

Certain materials must be added to provide a new and desirable property that was not originally present, to enhance a desirable property already possessed in some degree or to overcome some natural deficiency. Additives are used to reduce thermal and oxidative degradation, lessen the accumulation of harmful deposits, change the viscosity characteristics, minimize rust and corrosion, reduce wear, control frictional behavior, control foaming and prevent destructive metal-metal contact. Additives may be divided into two general types (a) those that modify some physical property such as pour point, foaming or viscosity-temperature behavior and (2) those that modify some chemical behavior such as oxidation corrosion and wear. Some of the additives from each class may be combined into multi-purpose additives for convenience or utility.

## 4.3 Adsorption of Lubricants

In boundary lubrication, a thin lubricant film is superimposed on the solid film whose shear strength is considerably less than that of the metal. Thus even in cases where strongly adsorbed films are present, their shear strength and sliding coefficient of friction cannot be very different from that of

the polymer itself. In this case, the bulk properties of the polymer may or may not be affected to some extent by the lubricant.

Definition of oiliness adopted by the Society of Automotive Engineers indicates the uncertainty which exists as to its actual origin. This definition describes oiliness as a term "signifying differences in friction greater than can be accounted for on the basis of viscosity when comparing different lubricants under identical test condition". Adsorption and lubricity characteristics are much more significant in the case of elastomers and polymers compared with metals. The long-chain molecular structure is not unlike that of the superimposed lubricant, for elastomers, so that adsorption may readily occur and the properties of the adsorbed film are similar to those of the elastomer. Accordingly, as we increase the chain length of the lubricant, it becomes increasingly difficult for the lubricant molecules to penetrate the polymer, and the lubricity or slippery effect deceases.

# CHAPTER 5

## FRICTION AND POWER LOSSES IN JOURNAL BEARING

It is usually possible to design a journal bearing to operate by fluid lubrication film and still carry a substantial load. Under these conditions, the friction losses in the bearing are generally very low and if the lubricant is free of abrasive matter, wear becomes vanishingly small.

### 5.1 Friction Loss On The Bearing

The difference in friction torque between bearing and journal can be evaluated in terms of the applied load and the eccentric distance between the center of the shaft and the center of the bearing. In Figure 5.1, the journal is eccentric in the bearing. Reaction of the load is through the center of the shaft, load act through the center of the bearing. The eccentric distance oo′ equals the radial clearance multiplied by the eccentricity ratio.

Thus oo′ = emr

Also two forces W act on oil film and create an amount since they are separated by distance oo′cosθ′.

$$Mc + Wem \cos\theta = Md$$

Mc: Is the friction moment of bearing acting on the oil film.

W: Is the force act in oil film.

Md: Is the friction moment of journal acting on oil film "if we consider it a free body".

emr: Is the distance between two forces W equal oo'cose as shown from Figure 5.1.

The actual friction losses in journal bearing are determined by the friction on the journal.

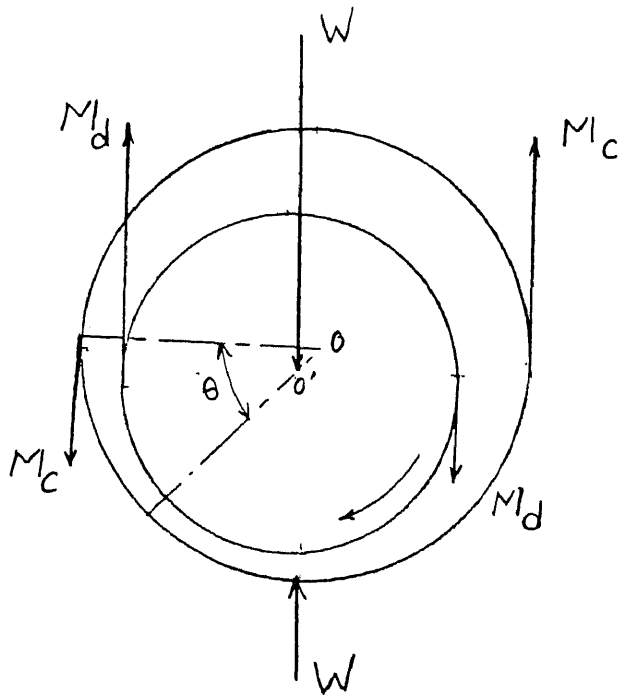


**Figure 5.1** Analysis of bearing torque and friction torque in a journal bearing.

### 5.2 Heat Balances in Self-Contained Bearing

In order to estimate the actual film temperature minimum film thickness, load-carrying capacity and friction loss, a balance must be established between the heat generated within the bearing and the heat dissipated from the bearing. Most industrial bearings are self-contained and are capable of getting rid of heat by conduction, convection and radiation to the surrounding atmosphere. In most machines, like motors, generators, turbines and pumps, they use pedestal bearing types.

Because such bearings reach equilibrium (from one to three hours after starting the machine), and there is also sufficient radiation and convection of the temperature of the bearing housing, this convection and radiation of temperature dissipates continually all the heat generated by friction in the bearing.

Operating at high speeds and heavy loads, equilibrium may be reached at high level of temperature, perhaps higher than 200 degrees F . That is why such conditions would not be acceptable for industrial use for two reasons. First, temperatures in excess of 200 degrees F initiate softening of the bearing metals themselves. Second, high temperatures cause a rather rapid deterioration of the lubricant itself, such as the chemical breakdown and the formation of harmful acids.

Also there is limit of acceptable equilibrium film temperature for the usual industrial application range from

160 to 180 degrees F. In case the temperature goes above the limit, there is simply a forced draft of air blowing over the bearing housing by using an ordinary electric fan. For more serious conditions, a cooling coil in the oil sump may be quite adequate. In the case of extreme conditions of heating, forced-feed oiling will be required with the hot oil being drained to separate reservoir where it may be cooled.

### 5.3 Minimum Oil-Feed Requirements to Maintain A Fluid Film in Journal Bearing

As we know, there is a limit if the oil supply diminishes and the film gets thinner. That limit is established when the film becomes so thin that the peaks of surface roughness exceed the minimum film thickness and begin to produce incipient metallic contact.

The magnitude of this minimum film thickness will depend upon the size and rigidity of the bearing housing and the surface finish of bearing and shaft.

To measure oil-feed rates in terms of cubic inches per second, you must know drop per minutes and the volume of the drop. On average for lubricating oil, we consider that 30 drops of oil have a volume of one cubic centimeter.

# CHAPTER 6

# EXPERIMENTAL PROCEDURE

## 6.1 Apparatus

In order to provide empirical verification of the dynamic friction model, an electro-mechanical friction testing system was developed. The experimental testing system (see Figures 6.1 and 6.2) is comprised of a testing apparatus fixture, personal computer, data acquisition and control interface board, digital strain indicator and a collection of analog signal amplifiers and D.C. power supplies. The test fixture itself contains a main support frame, shaft-bearing assembly, shaft loading assembly, servo-motor, tachometer (D.C. motor), strain gage mounting strips and a shaft loading assembly lubrication system.

Design features of the apparatus are explained with the aid of Figure 6.1. The journal test-shaft (C) is supported by two roller bearings (A) attached to the main support frame (B). There are four brass test-loading sleeve bearings (H). The clearance between the journal and each sleeve bearing is 0.001 in. The adjustable load is applied by tightening the nut (P) on bolt (R). This causes the two center test-bearings and the two outer test-bearings to be loaded equally and in opposite directions, (action and reaction forces) thereby applying equal forces between journal and each bearing. The electric servo-motor (U) is connected to

the main support frame with an adjustable motor-mounting bracket

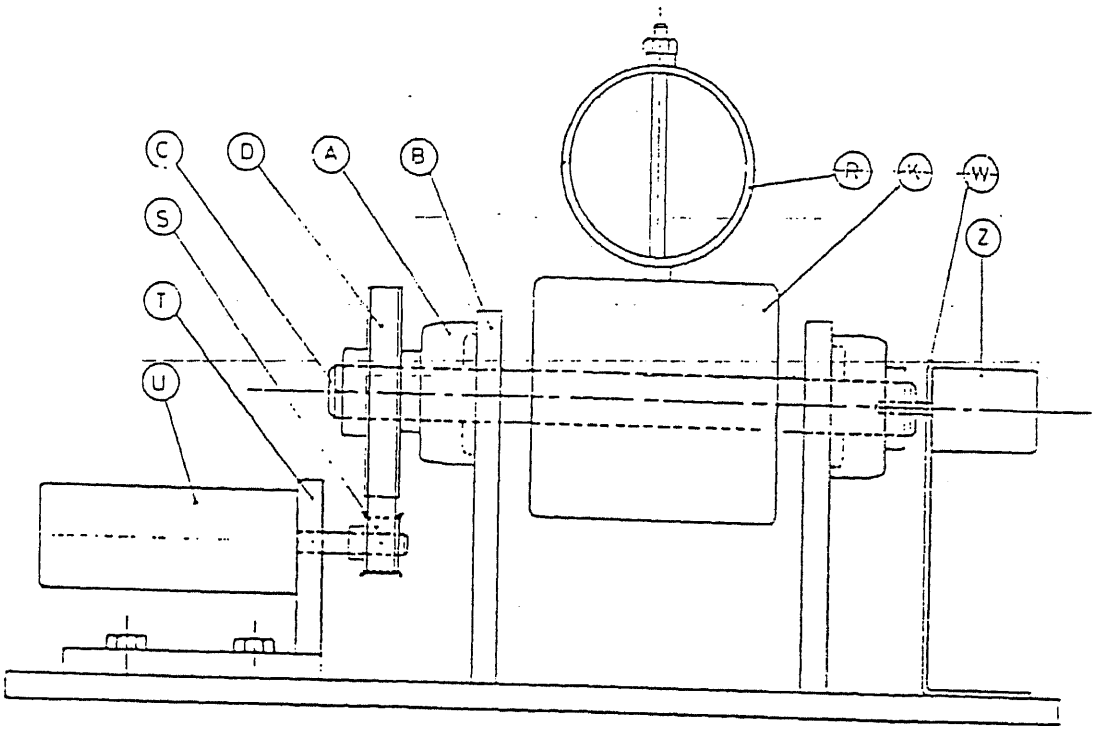


**Figure 6.1** Overall mechanical system

(T). A timing V-belt and two pulleys (D & S) transfer the motion of the servo-motor to the test-shaft. The number of shaft

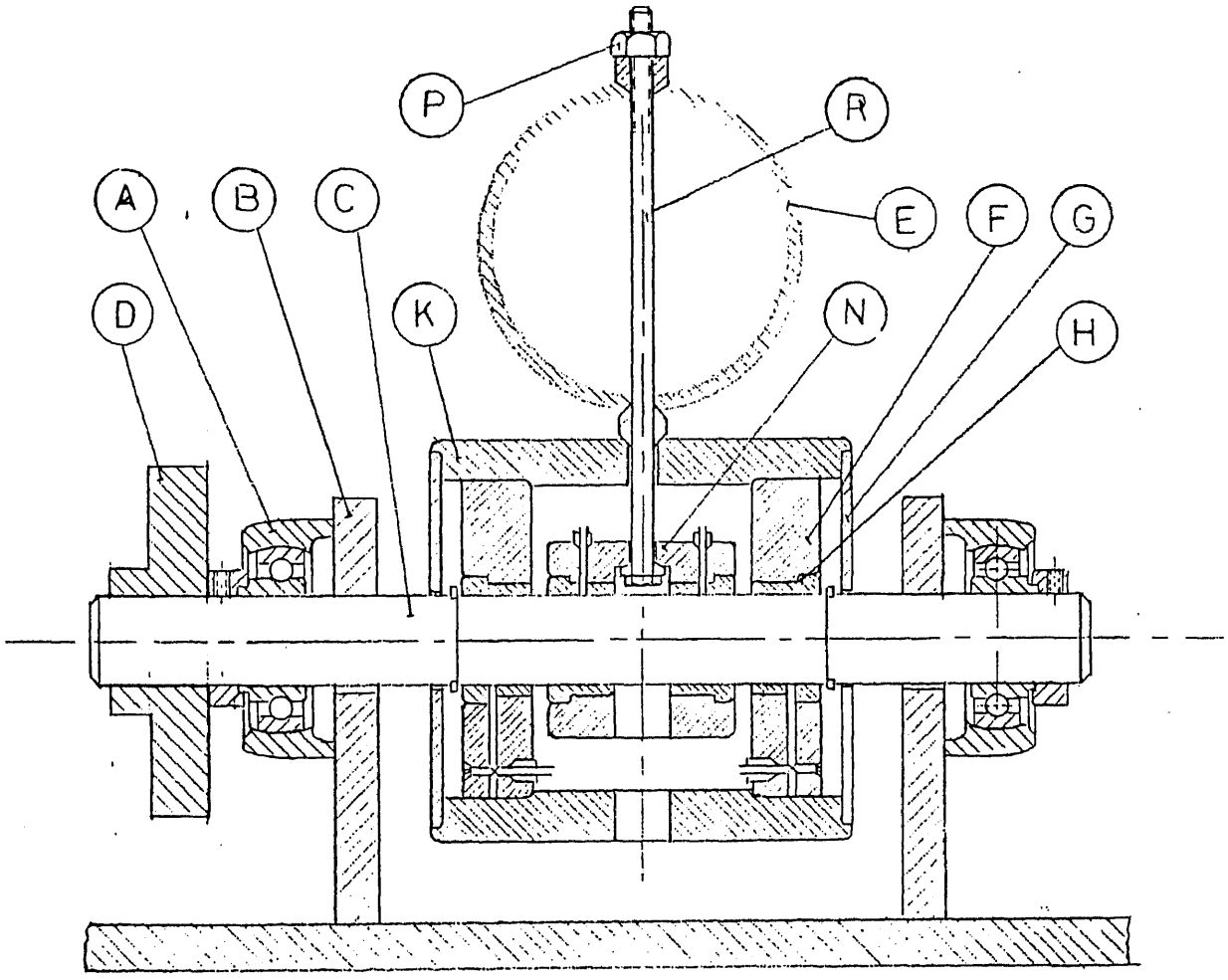


**Figure 6.2** Cross-sectional view of friction system

pulley grooves is four times the number of grooves on the servo-motor shaft pulley (S) in order to reduce the test-shaft speed to one-quarter of the servo-motor speed and to increase the torque transmitted to the test-shaft. Lubricating oil is delivered into the clearance between the sleeve and journal through four segments of flexible plastic tubing. A lubricating oil reservoir pan is mounted at the top of the test-fixture. Expelled oil from the shaft loading assembly accumulates in an oil-collecting pan located below the shaft-loading-assembly and drains into a larger collection vessel through the provided outlet pipe.

### 6.2 Experimental Apparatus Test Logic (General)

The experiment entails using a servo-motor to drive the test-shaft with a pre-determined voltage wave form which induces a specific motion in the shaft-loading-assembly. This motion is transferred by the two shaft-loading-assembly support members to the two strain-gage mounting strips. The resulting strain in the mounting strips is sensed by a strain-gage full bridge configuration. The full bridge output and test-shaft tachometer velocity signals are processed and finally recorded by the computer system. These recorded values are used to render a graph of Friction Torque vs. Shaft Velocity. This experimental data is later compared to the results generated by the theoretical simulation model.

## 6.3 Main Cylinder (K)

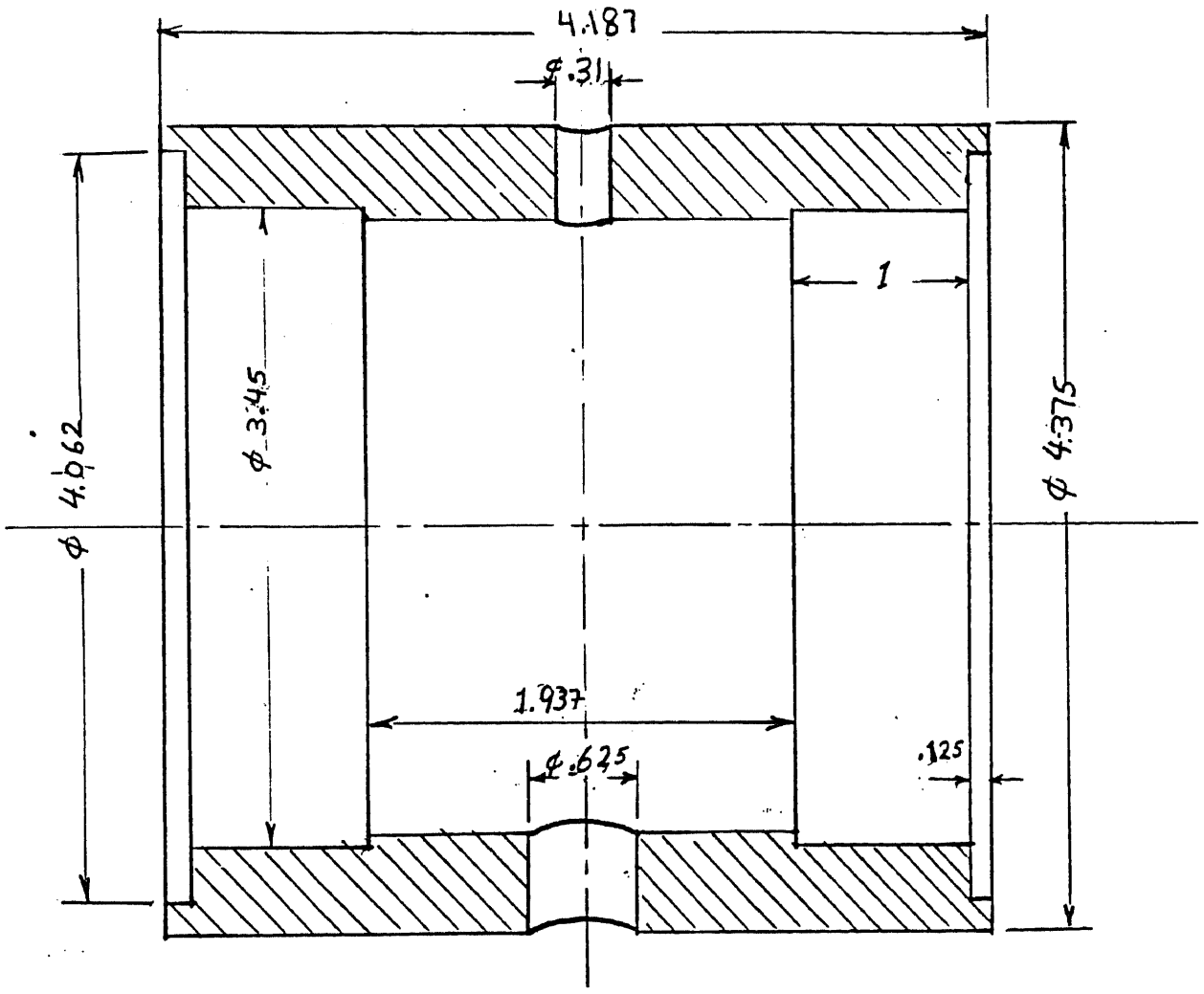


**Figure 6.3** Main Cylinder

The main cylinder is made from steel. Its dimensions are 4.43 inches on the outer diameter, 3.45 inches on the inner diameter and 4.26 inches long. In the middle of this cylinder is a 0.312 inch hole drilled from the top and a 0.625 inch hole drilled from the bottom. The purpose of the larger hole on the bottom and the smaller hole on the top is to allow the bolt to extend upward through the cylinder and the lubricating pipe to go through the bottom hole.

**6.4 Small Cylinder**

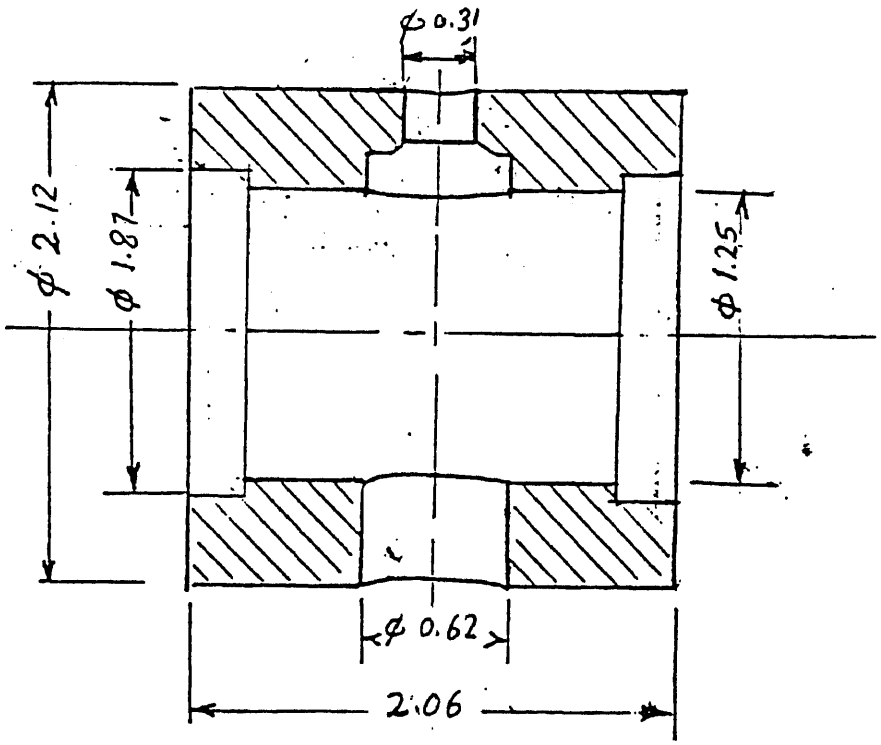


**Figure 6.4** Small Cylinder

The small cylinder is made from steel. Its dimensions are 2.125 inches outer diameter, 1.375 inches inner diameter and 2.062 inches long. In the middle of this cylinder a 0.312 inch hole is drilled on the top of this cylinder. Also a 0.625 inch hole is drilled on the center of the bottom side, two loading-bearing (H) are press fit inside this cylinder. The movement of the head of the bolt is controlled by the narrowing diameter of the top hole.

**6.5 Test-Loading Bearing (H)**

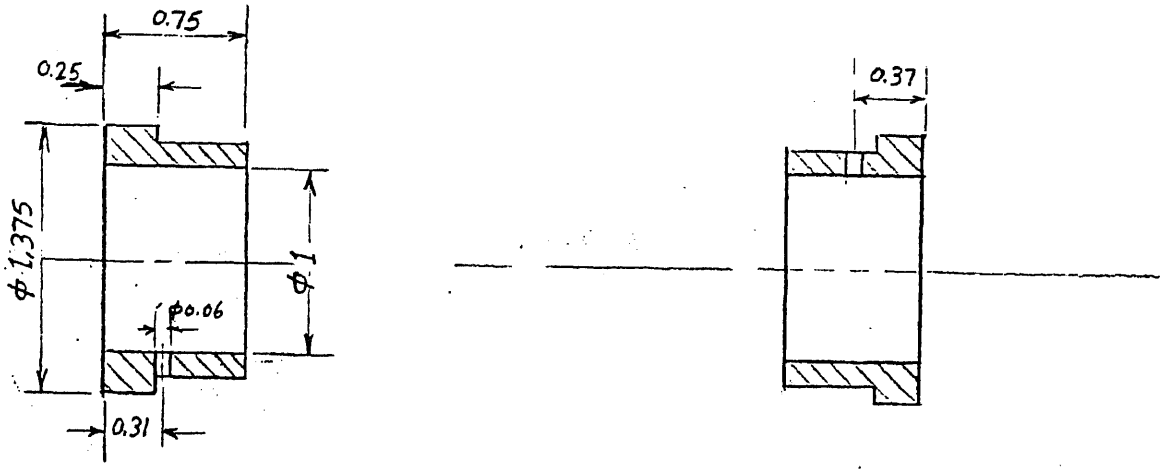


**Figure 6.5** Test-loading bearing

This bearing is made from brass. It has an 1.375 inch outer diameter, a one inch inner diameter and is 0.75 inches long. In this machine, we use four pieces from test loading-bearing, each one is mounted inside steel bushing and then a 0.18 inch hole is drilled through both bearing and bushings for the lubricating oil.

### 6.6 Thin Ring

The classical case of a thin ring loaded in the plane of curvature represents a statically indeterminate problem. This seems somewhat surprising considering the regularity of the geometrical shape and structural response.

The equilibrium of forces for one quadrant of the ring is essentially the same for both tension and compression and the problem is simplified considerably when symmetry of loading and support is observed. The decrease in the vertical diameter obtained by the formula

$$W = ybE/x\ (1.7856X^2 + 2.8207) \qquad (6.1)$$

where

E:Modulus of elasticity, psi.

b:Width of rectangular section, in.

W:Concentrated load, ib.

R:Mean radius of curvature, in.

Y:Vertical deflection, in.

h:Thickness of the ring, in.

X=R/h

The thin steel ring (E) as shown in Figure (2) is about three

inches in diameter and 0.006 inches in thickness; end of a long steel bolt which end by nut (P) goes through this thin ring to apply the friction force by tightening the nut (P) on the bolt (R).

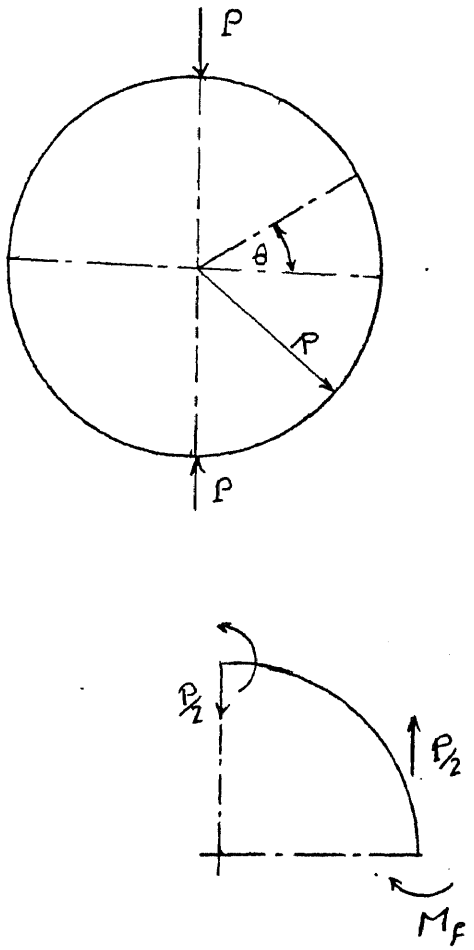


**Figure 6.6** Equilibrium of force for thin ring

## 6.7 Strain Gage Strip

The initial step in preparing for any strain gage installation is the selection of the appropriate gage for the task. It might at first appear that gage selection is a simple exercise of no great consequence to the stress analyst; but quite the opposite is true. In this machine, we use four strain gages, two strain-gage mounting strips; one on each side of the big cylinder. Each mounting strip is held from one side by one bolt and it is free from the other side. Two strain gages are mounted on each strip, one on the top and one on the bottom.

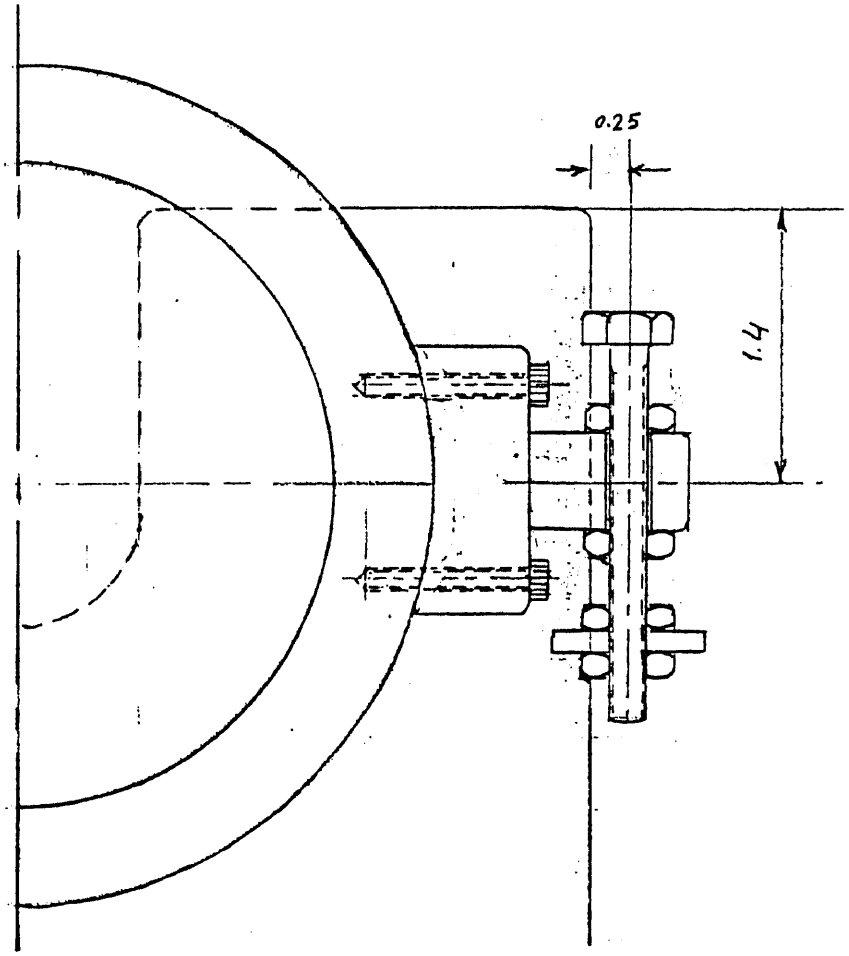


**Figure 6.7** Strain gage system

### 6.8 Main Frame

This frame is made from aluminum. Its dimension are 18 inches long, 6 inches wide with a 0.5 inch thickness. In the right side of this base we mounted two vertical supports, 6 inches wide and 6.75 inches in height. On top of the middle of each vertical support we made a top cut with dimensions of 1.25 inches wide and 1.5 inches in depth and we fixed two-bolt flanged bearings in each side to hold the main shaft (C) as shown in Figure (b). In the left side of the main frame we cut two slots to mount the servo-master base by four bolts into the main fame.

## CHAPTER 7

## DATA ACQUISITION

The requirement for a method of precise motion control of machinery in closed-loop control systems under conditions of time-varying velocity provided the motivation for current investigation. Data acquisition is explained with the aid of

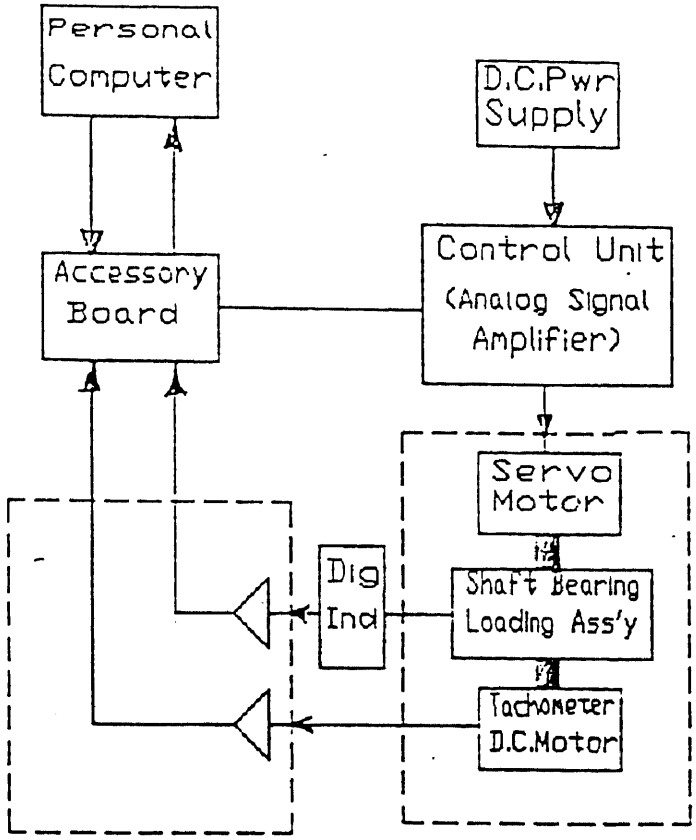


**Figure 7.1** System block diagram

igure 7.1 which shows us system block diagram which consists f a test fixture. This was explained in Chapter 4, personal omputer, digital strain indicator and a collection of analog ignal amplifiers and D.C. power supplies.

## 7.1 Personal Computer

*omputer Type*

n this machine we use 486DX IBM compatible personal computer ith MS.DOS 6. In this computer we used MetraByte's model ASH-16F which is multi-function high speed analog/digital I/O xpansion boards for the IBM or the compatible computer.

*oftware*

n this machine we used VisSim, which is the powerful omputer-aided engineering (CAE) program that provides a omplete visual and graphical work space for designing, imulating, and plotting models of dynamic system.

In VisSim we can build models in the form of block iagrams.

Blocks and flex wires are the primary design tools. Wire locks together assign appropriate block and simulation arameters, simulate the diagram and plot the results, all ithin single interactive environment.

*ardware Installation*

ASH-16/16F utilizes 16 consecutive address locations in I/O pace. Some I/O addresses will already be used by internal

I/O and your other peripheral cards, so to avoid conflict with these devices, DASH-16's I/O address can be set by the BASE ADDRESS D.I.P. switch to be on a 16 bit boundary anywhere in the I.B.M. PC decoded I/O space. The P.C.'s expansion I/O address space extends from decimal 512-1023 (Hex 200-3FF) which is much greater than is ever likely to be fully occupied.

This covers the standard IBM I/O options (most compatibles are identical). but if you have other I/O peripherals e.g. special hard disk drives, special graphics boards, prototype cards etc. they may be making use of I/O addresses not listed in the table above. Memory addressing is separate from I/O addressing so there is no possible conflict with any add-on memory that may be in your computer.

Usually, a good choice is to be put the DASH-16/16F at base address Hex &H300 (Decimal 768 or 784). As an aid to setting the base address D.I.P. switch, a graphical switch position display program, INSTALL.EXRE can be run from the DOS prompt. This program also will generate a DASH16.ADR file that holds the DASH16/16F I/O address for the use of other programs. To run the installation aid program, type:

A:> INSTALL

When you get the "Desired base address?" prompt, type in your choice in decimal or IBM &H --- format and press return. The program will round your address to the nearest 16 bit boundary, check for possible conflicts with standard IBM I/O devices and draw a picture of the correct positions of the

toggles on the base address DIP switch.

INSTALL.EXE performs one further optional function. You can generate a file named DASH16.ADR which contains the base I/O address that you have selected. If your application programs read this file instead of declaring, the address in each program (list EXO.BAS to see how it's done), then should you wish to change the board address in the future, all you have to do is alter the DASH16.ADR file instead of altering dozens of application programs. Your DASH-16 disk comes with a DASH16.ADR file ready loaded with decimal 768 (Hex 300) which will be overwritten if you choose to generate another address file when you run INSTALL.

The next step is to remove the DASH-16/16F board from its protective electrostatic packaging and set the BASE ADDRESS dipswitch located just to the upper left of the gold edge connector. It is a good precaution to discharge any electrostatic charge you may have accumulated by touching the metal frame of your computer before inserting the board in the computer. This is also a convenient point to set some of the other switches on the DASH-16 board if you wish (it is not essential at this stage). Their functions and markings are as follows:

1. CHAN CNFG (Channel configuration). Decide whether you want 8 differential or 16 single ended analog input channels and set this slide switch on in the 8 or 16 position accordingly.

2. A/D. This slide switch controls the input range. In

the UNI (unipolar) position inputs can be positive only i.e. ranges are from zero to some positive full scale voltage. In the BIP (bipolar) position, inputs can range from equal negative to positive full scale limits.

3. DMA. This slide switch selects the operating DMA level. If you have floppy disk drives only on your computer (plain IBM P.C. set it to level 3. If you have a hard disk equipped computer (P.C./XT or equivalent), level 1 is preferable, although operation of some hard disk equipped machines may also be possible on level 3.

4. GAIN. There are 2 different DASH-16 board designs. Those bearing the number PC-6102 have a 6 position dipswitch. Only one slider of this DIP switch should be in the ON position. This controls the input scaling as follows:

| GAIN | UNIPOLAR | BIPOLAR |
|---|---|---|
| 0.5 | N/A | +/-10v |
| 1 | 0 - +10v | +/-5v |
| 2 | 0 - +5v | +/-2.5v |
| 5 | 0 - +2v | +/-1v |
| 10 | 0 - +1v | +/-0.5v |
| USER | | |

The second design bears the number PC-6542 and has a 5 position dipswitch marked A, B, C, D, USER that sets the ranges as follows:

| A | B | C | D | USER | UNIPOLAR | BIPOLAR |
|---|---|---|---|---|---|---|
| OFF | OFF | OFF | OFF | OFF | N/A | +/-10V |
| ON | OFF | OFF | OFF | OFF | 0 - 10v | +/-5v |
| ON | ON | OFF | OFF | OFF | 0 - 5v | +/-2.5v |
| ON | OFF | ON | OFF | OFF | 0 - 2v | +/-1v |
| ON | OFF | OFF | ON | OFF | 0 - 1v | +/-0.5v |
| ON | OFF | OFF | OFF | ON | *User set *See section 9.2 | *User Set |

Additional graphical assistance in setting the range

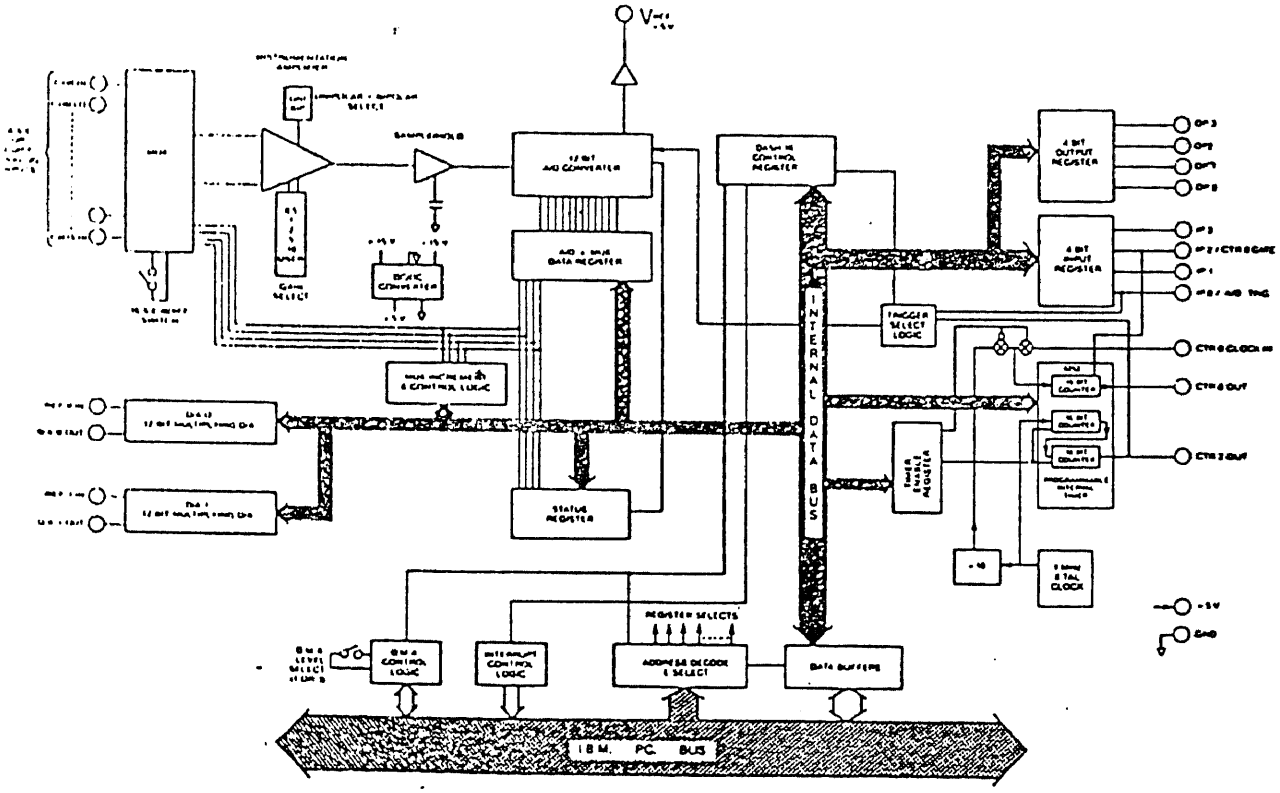


**Figure 7.2** Block diagram of DASH-16116F

switch can be obtained by running the CAL.BAS (for PC-6102) or CALF.BAS (for PC-6542) calibration programs and selecting the A/D converter calibration option. None of the above switch settings apart from the BASE ADDRESS is critical to operation of the board.

To install the board, TURN OFF THE POWER on your computer and remove the case. Remove a vacant back plate by undoing the screw at the top and plug the DASH-16/16F in and secure the backplate. DASH-16/16F will fit in any of the regular full depth slots of the IBM P.C. ir X.T. or Portable computer. On the PC/AT, it can be plugged into any socket but it will not make use of the extended AT bus interface connector. Installation is now complete. You may plug any of the DASH-16 accessories or your own cable into the 37 pin D connector on the rear.

### 7.2 Digital Strain Indicator

In this machine we measure the deflection by using four strain gage, two in each side to determine numerically the strain in a structure or the output of a transducer with this Digital Strain Indicator. We can get:

. Direct reading LED display reading +/-1999 counts (+/-19999 with option M) representing microstrain with a resolution of lue (and +/-19,990 ue with 10 ue resolution).

. Ultra-stable amplifier with near-zero drift.

. Wide-range span control (approx. 40:1) achieved by varying bridge excitation with a constant-current power supply.

. Bridge completion circuits for half-bridge and 120 or 350 ohm quarter-bridge operation (3-wire) operation.

. Built-in shunt-calibration circuit to simulate 1000 ue at GF=2 in half-or quarter-bridge operation (any resistance).

. Extreme immunity to electrical noise on the input.

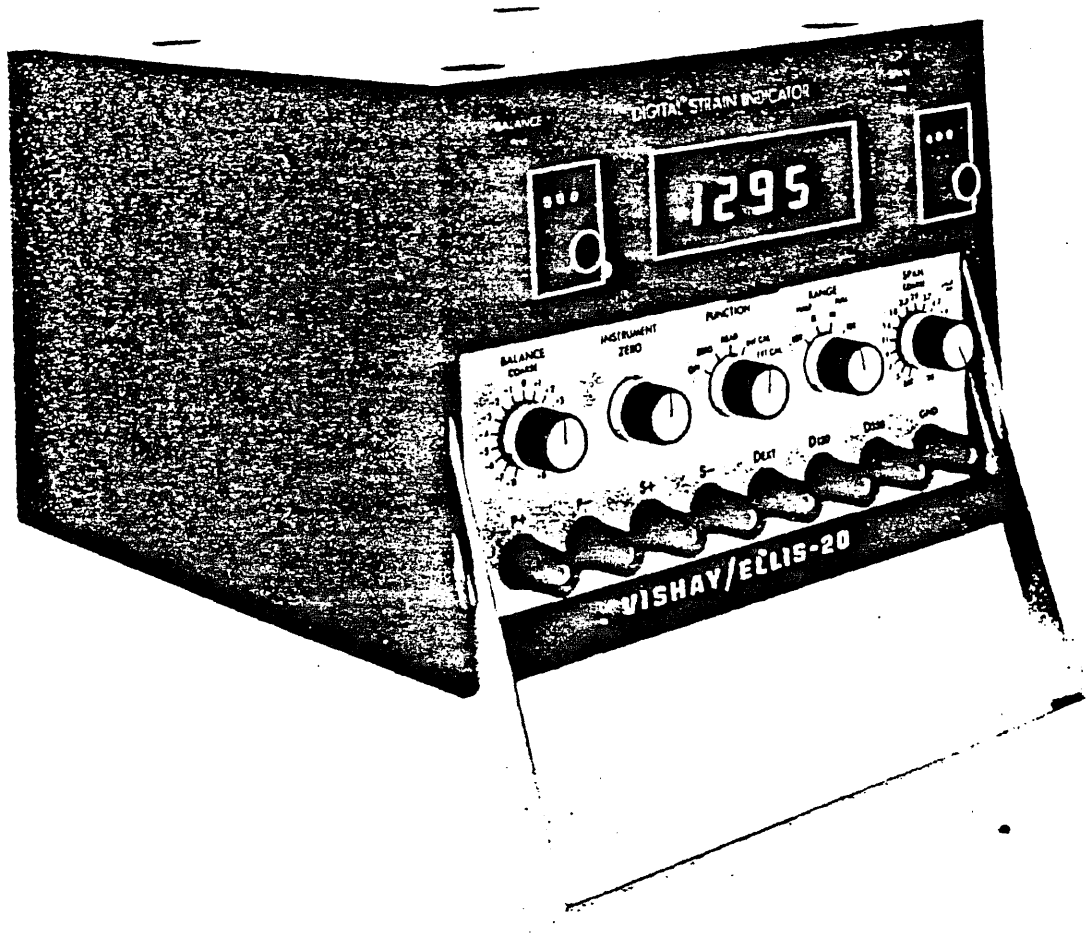


**Figure 7.3** Strain gage indicator

*Line Power*

On the Front Panel, place the FUNCTION switch at OFF.

At the rear of the instrument, set line voltage switch to proper setting, 115 or 230 Vac. Remove line cord from cord-wrap. Insert narrow (female) end into oval receptacle (this receptacle is polarized, and plug will only go in one way - do not force it). Insert 3-prong plug at opposite end of line cord into the appropriate 50-60Hz grounded power receptacle.

NOTE: If the standard plug must be replaced by a different type, use the following color code: black to hot, white to neutral, and green to ground (earth),

On the Front Panel, turn the FUNCTION switch to ZERO and the RANGE switch to X1 (either HALF or FULL depending on the intended input circuit).

The Display should light and read near 000. Normally, no adjustment of this reading would be made until the input wiring is complete (following steps).

*Input Connections*

Connect the input to the instrument. Note that the "tension" or "compression" designation simply indicates the direction of strain at the gage position which will yield a positive reading at the Display.

IMPORTANT: The amplifier inputs operate at a quiescent level which is several volts dc above instrument ground. Consequently the input circuit (gages) must be very well insulated from any ground.

Normally the input wiring is connected to the binding posts on the front panel, However, the circular INPUT connector at the rear of the instrument picks up wires from all binding posts and can be used as an alternate input.

### 7.3 Strain Gage

Careful, rational selection of gage characteristics and parameters can be very important in: optimizing the gage performance for specified environmental and operating conditions, obtaining accurate and reliable strain measurements, contributing to the ease of installation, and minimizing the total cost of the gage installation.

The installation and operating characteristics of a strain gage are affected by the following parameters, which are selectable in varying degrees:

. strain-sensitive alloy

. backing (carrier) material

. gage length

. gage pattern (number, arrangement, and orientation of grids; grid width; solder tab type and configuration; etc.)

Considering all possible combinations of the above parameters, the strain gage selected for a particular application then represents a choice of one out of some 50,000 types available from Micro-Measurements. Basically, the gage selection process consists of determining the particular available combination of parameters which is not compatible with the environmental and other operating conditions, and at

the same time best satisfies the installation and operating constraints.

*Strain-Sensing Alloy*

The principal component which determines the operating characteristics of a strain gage is the strain-sensitive alloy used in the foil grid. However, the alloy is not in every case an independently selectable parameter. This is because each of Micro-Measurements strain gage series is designed as a complete system, comprised of the foil and backing, and usually certain other construction features particular to that series.

*Backing Material*

Conventional foil strain gage construction involves a photoetched metal foil pattern mounted on a plastic backing or carrier. The backing serves several important functions:

. provides a means for handling the foil pattern during installation

. presents a readily bondable surface for cementing the gage to the test specimen

. provides electrical insulation between the metal foil and the test object

The backings supplied on Micro-Measurements strain gages are of three basic types: polyamide, epoxy, and glass-fiber-reinforced epoxy-phenolic.

*Gage Length*

The gage length of a strain gage is the active or strain-sensitive length of the grid, as shown in Figure The end loops and solder tabs are considered insensitive to strain because of their relatively large cross-sectional area and low electrical resistance.

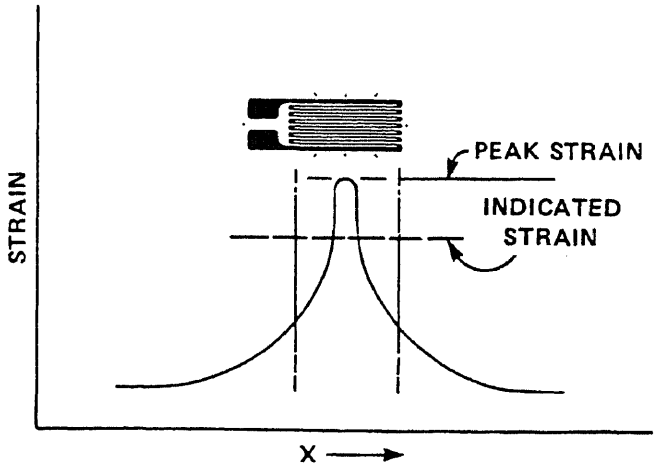


**Figure 7.4** Strain gage length

Gage length is an important consideration in strain gage selection, and often the first parameter to be defined. For example, strain measurements are usually made at the most critical points on a machine part or structure - that is, at the most highly stressed points. And, very commonly, the highly stressed points are associated with stress concentrations, where the strain gradient is quite steep, and the area of maximum strain restricted to a very small region. Since the strain gage tends to integrate, or average, the strain over the area covered by the grid, and since the average of any nonuniform strain distribution is always less than the maximum, a strain gage which is noticeably larger than the maximum strain gage region will indicate a strain magnitude which is too low.

*Strain Gage Used*

A strain gage which consists of a protective encapsulation of polyamide film approximately 0.001 in (0.025mm) thick, which covers the entire gage except for a portion of the folder tabs. This combines ruggedness with excellent grid protection, at no sacrifice in flexibility, Soldering is greatly simplified since the solder is prevented from tinning any more of the gage tab than is deliberately exposed to lead attachment.

Option E contributes significantly to long-tern stability because the grid cannot be contaminated by fingermarks or other corrosive agents during installation. Supplementary

protective coatings should still be applied after lead attachment in most cases.

When gages are properly wired with small-diameter jumpers between gage tabs and terminals, maximum endurance capability under fatigue conditions is easily obtained. Heavier loads can be attached directly to the gage tabs for simply static load tests.

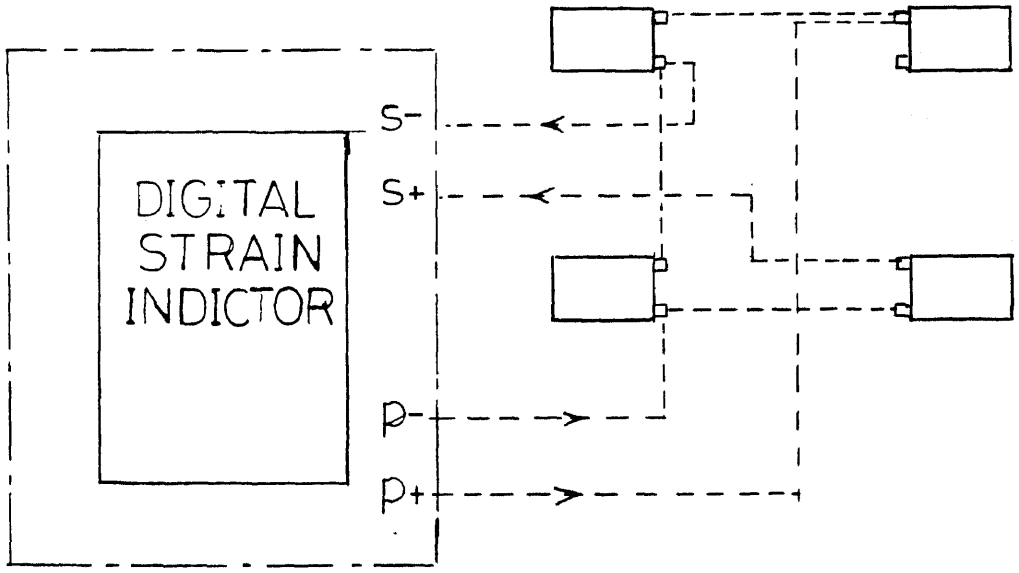


**Figure 7.5** Connection of strain gage with digital strain indicator

# CHAPTER 8

## EXPERIMENT RESULTS

The dynamic effects of friction are particularly significant in control systems, in which the effect of friction can significantly impact on the performance of the system. Although friction always results in dissipation of energy, its effect on the feedback control system can be either stabilizing or destabilizing, depending on where the friction appears and on the measures, if any, taken to overcome its effects.

In (Figure 8.1) the transition velocity Utr, in the Stribeck curve, shows the mixed lubrication region where the thickness of the lubrication film is less than the maximum size of the surfaces, resulting in elastic as well as plastic deformation of the asperities. The external lead is carried partly by the pressure of the hydrodynamic fluid film and partly by mechanical elastic reaction of the deformed asperities, in the mixed region.

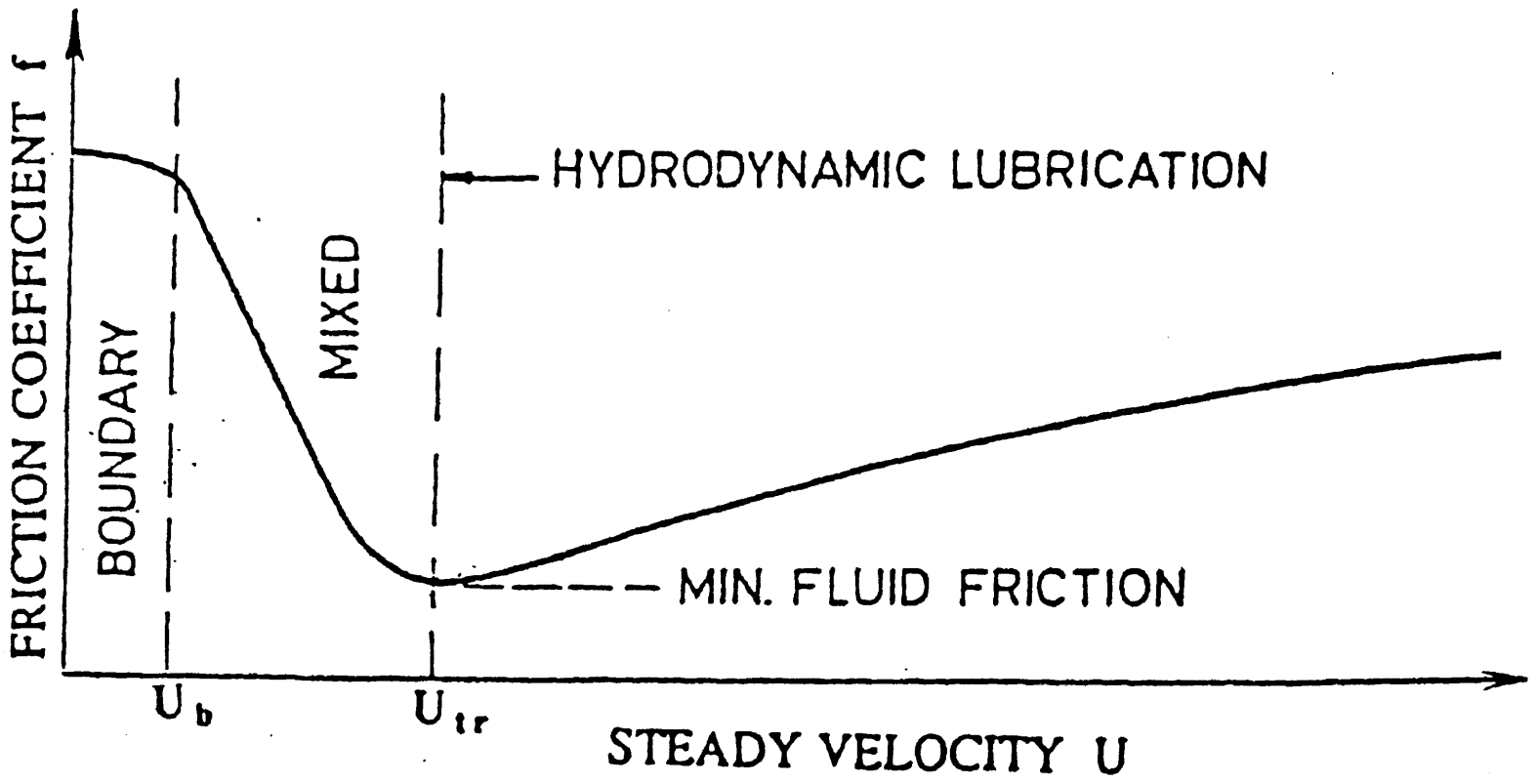


**Figure 8.1** Stribeck curve

Under the classical hydrodynamic lubrication theory, the lubrication film thickness increases with velocity. Figure 7.1 shows the well known Stribeck curve of friction coefficient versus steady sliding velocity between lubricated sliding surfaces, including hydrodynamic journal bearings. Below the transition when the sliding velocity is above the minimum critical velocity, Utr, the region of full hydrodynamic lubrication occurs. In this region there is only a viscous friction between the sliding surfaces. The viscous friction increases with velocity because the shear rates and shear stresses are proportional to the sliding velocity.

The dynamic friction under oscillating velocity shows a hysteresis effect. The instantaneous friction is higher (compared with the steady friction) when the friction force is rapidly decreasing, due to increasing velocity and lower when the friction is rapidly increasing, due to decreasing velocity. In Figure 8.2, theoretical results show that the friction at zero velocity is less than the maximum friction and maximum friction as well as that at zero, are decreasing with the frequency ratio oc.

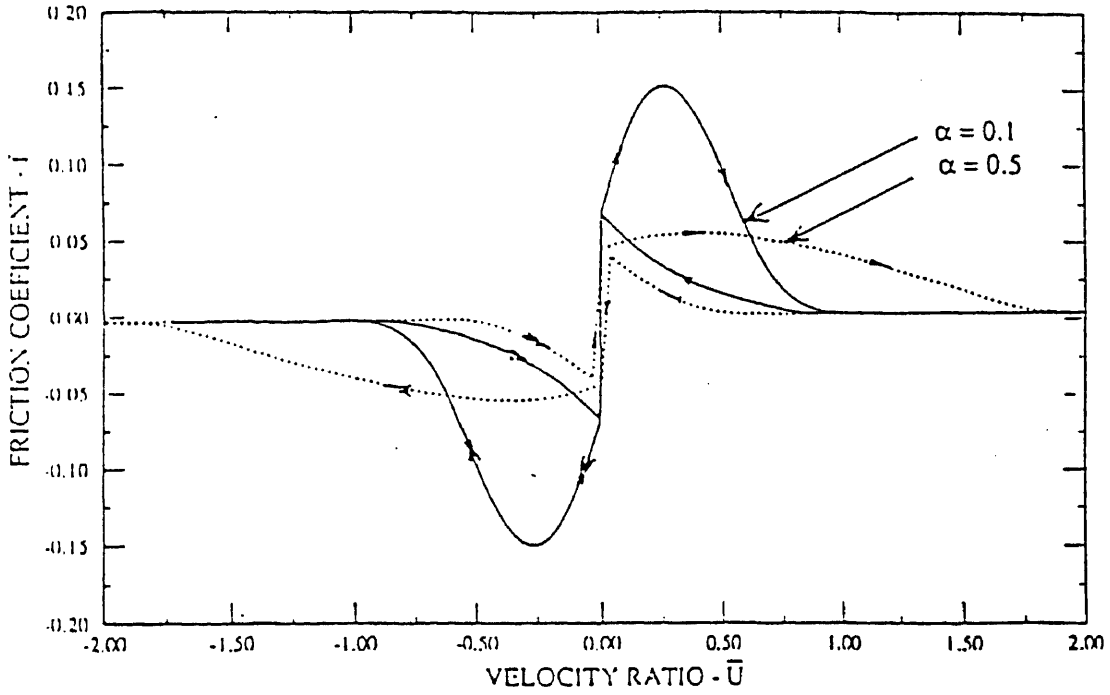


**Figure 8.2** Dynamic friction coefficient curves, for oscillating velocity U=2.0 sin 2t and the mass m=100, for various frequency ratio oc.

To run the experiment, we have to do the following:

- Make sure the oil goes into the machine by gravity.
- Make sure that all wires are properly connected.
- Adjust the digital strain indicator to zero reading.
- Turn PC computer on and start the Microsoft Windows.
- Double-click on the VisSim icon.
- Point to File in the menu bar and click the mouse.
- Select experiment file from the File menu.

Set the time, cycle and amplitude to run experiment.

To calculate the load "W" on the thin ring, we will use this formula:

$$W=ybE/X\ (1.7856X^2 + 2.8307) \qquad (8.1)$$

where:

W: is vertical load, (N)

y: Vertical deflection in thin ring, (mm)

b: Width of rectangular section, (mm)

E: Modules of elasticity, ($N/mm^2$)

X: Ratio of radius of curvature to depth of section

X = R/h

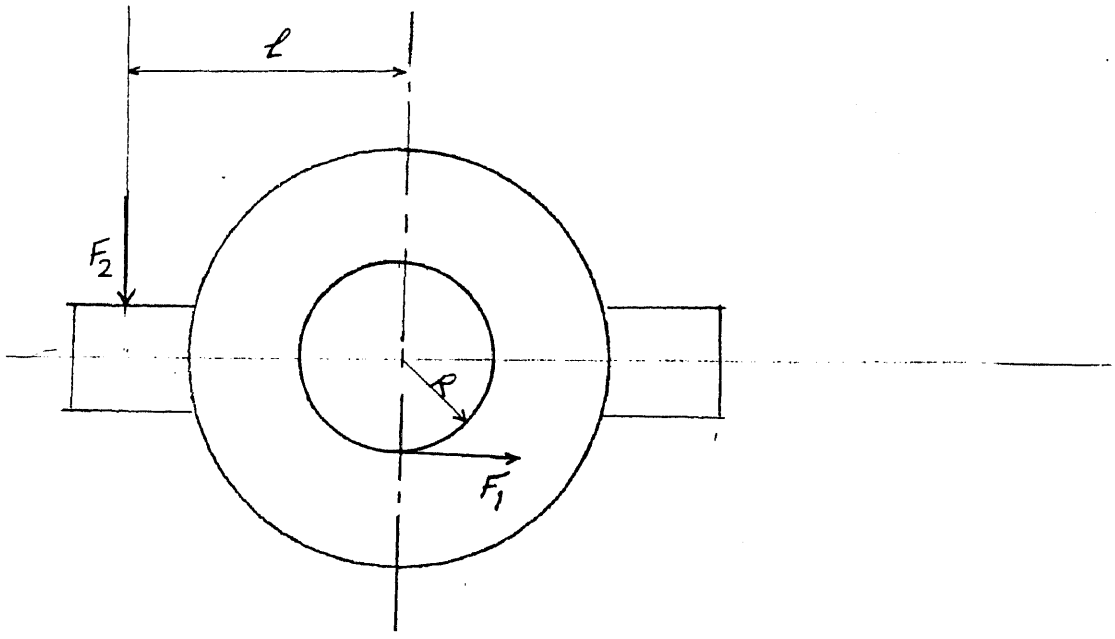


**Figure 8.3** Friction torque in the machine

To calculate the friction force on the bearing, we use the formula

$$lF2 = RF1 \qquad (7.2)$$

$$F1 = lF2/R \qquad (7.3)$$

Since we know (reading force) F2 by calibrating the strain gage signal, then we can get (friction force) F1 from equation 7.3.

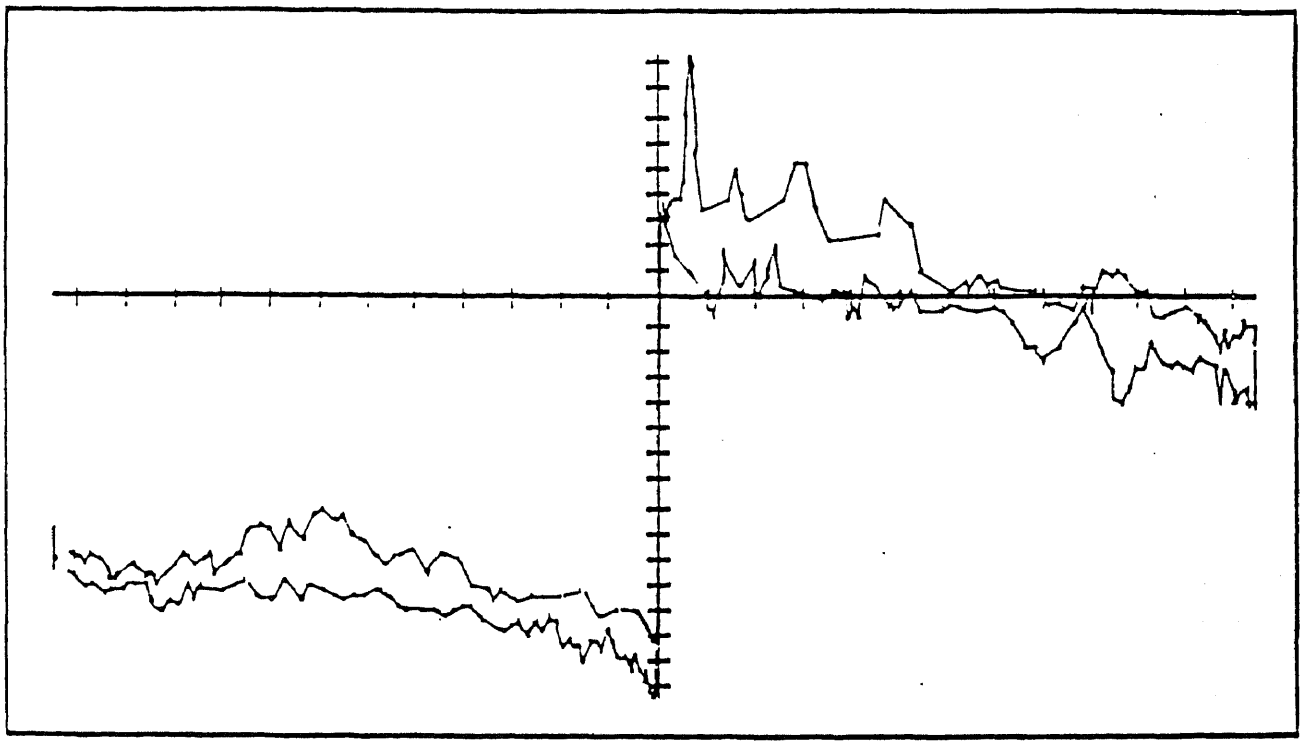


**Figure 8.4** Experimental result

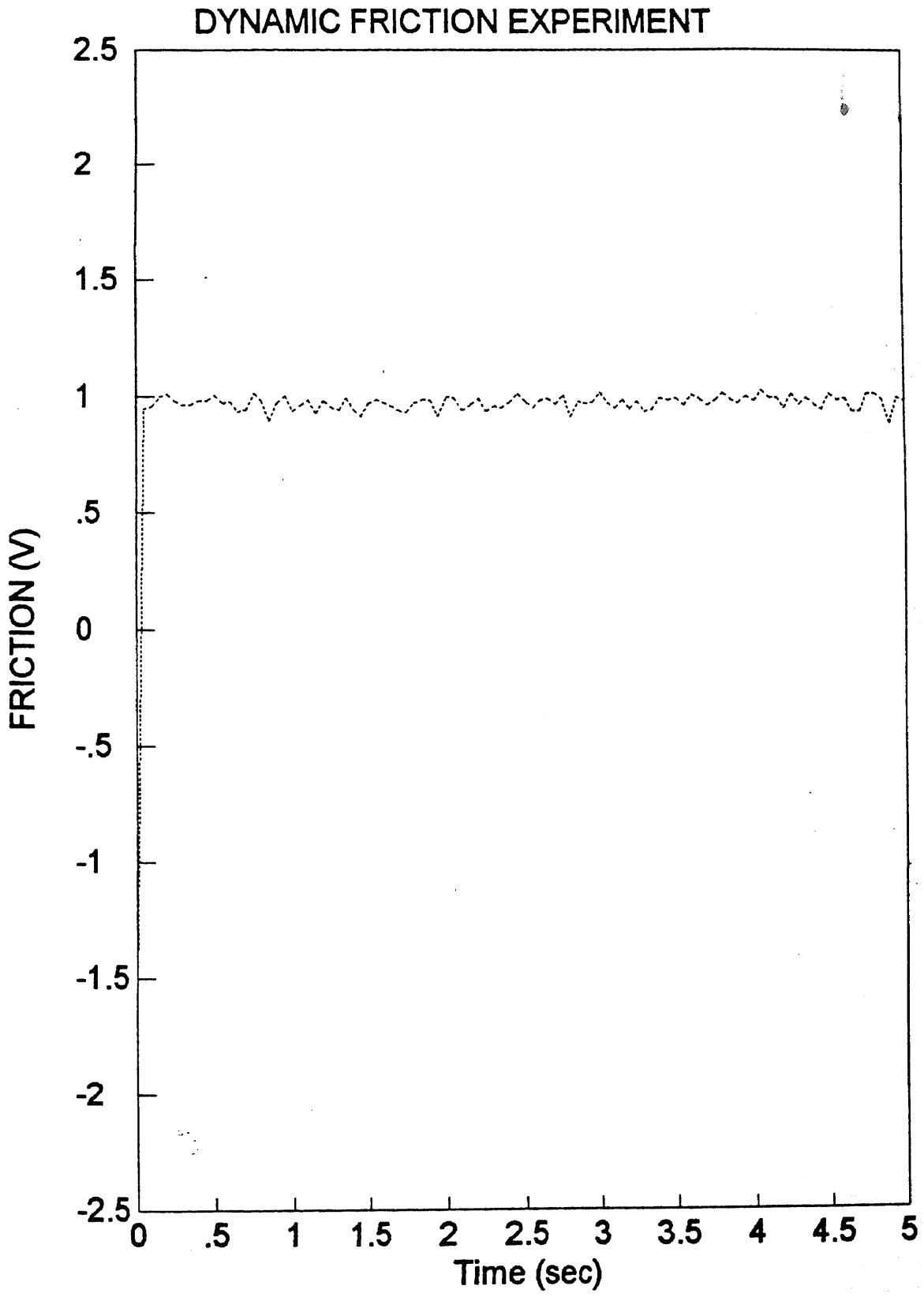


**Figure 8.5** Calibration curve

## REFERENCES


1. Felzenstein, Moshe. 1988. *"Hydrodynamic Lubrication Performance of Mineral Oils with Polymer Additives"*. Master Thesis - NJIT.

2. Fuller, Dudley, D. 1984. *"Theory and Practice of Lubrication for Engineers"*. New York. John Wiley

3. Harnoy, A. and Friedland, B. 1993. *"Dynamic Friction of Lubricated Surfaces for Precise Motion Contrc* Stleiasme. 93-TC.

4. Loewy, J., Harony, A. and Bar-Neji, S. 1972. *"Comp Bearing Rolling Element with Hydrodynamic Journal"* of Technology. Vol. 10, pp. 271-276.

5. Moore, Desmond. 1975. *"Principles and Applications Tribology"*. New York. Pergamon Press.